

See discussions, stats, and author profiles for this publication at: <https://www.researchgate.net/publication/231705324>

# Precisely and Irregularly Sequenced Ethylene/1-Hexene Copolymers: A Synthesis and Thermal Study

ARTICLE *in* MACROMOLECULES · MARCH 2009

Impact Factor: 5.8 · DOI: 10.1021/ma802241s

---

CITATIONS

34

---

READS

25

2 AUTHORS, INCLUDING:



Giovanni Rojas

University ICESI

28 PUBLICATIONS 256 CITATIONS

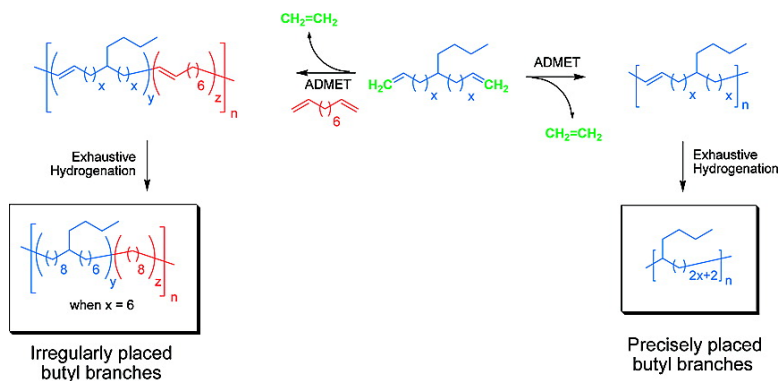
SEE PROFILE

## Precisely and Irregularly Sequenced Ethylene/1-Hexene Copolymers: A Synthesis and Thermal Study

Giovanni Rojas, and Kenneth B. Wagener

*Macromolecules*, **2009**, 42 (6), 1934-1947 • DOI: 10.1021/ma802241s • Publication Date (Web): 17 February 2009

Downloaded from <http://pubs.acs.org> on March 17, 2009



### More About This Article

Additional resources and features associated with this article are available within the HTML version:

- Supporting Information
- Access to high resolution figures
- Links to articles and content related to this article
- Copyright permission to reproduce figures and/or text from this article

[View the Full Text HTML](#)



**ACS Publications**  
High quality. High impact.

Macromolecules is published by the American Chemical Society, 1155 Sixteenth Street N.W., Washington, DC 20036

# Precisely and Irregularly Sequenced Ethylene/1-Hexene Copolymers: A Synthesis and Thermal Study

Giovanni Rojas<sup>†</sup> and Kenneth B. Wagener\*

Center for Macromolecular Science and Engineering, The George and Josephine Butler Polymer Research Laboratory, Department of Chemistry, University of Florida, Gainesville, Florida 32611-7200

Received October 7, 2008; Revised Manuscript Received January 16, 2009

**ABSTRACT:** Step-growth acyclic diene metathesis (ADMET) polymerization chemistry followed by exhaustive hydrogenation offers a new alternative in modeling ethylene/1-hexene (EH) copolymers. In contrast to chain-growth chemistry, this new approach produces well-defined, defect-free primary structures. This report describes the synthesis, characterization, and thermal behavior of ADMET-produced polyethylene materials containing either precisely or irregularly spaced butyl branches, the latter to serve as models for ethylene/1-hexene copolymers made via chain-growth chemistry. The thermal behavior of the new materials was studied using differential scanning calorimetry, and detailed NMR and IR analyses permitted the characterization of the primary structures. Properties of the here presented ethylene/1-hexene copolymers models can be varied from semicrystalline to fully amorphous by precise control of comonomer content and spacing.

## Introduction

Ethylene-based copolymers have been the most widely used thermoplastic materials for decades now,<sup>1</sup> with linear low-density polyethylene (LLDPE) playing an important role,<sup>2</sup> because of the diversity of materials that can be produced. The physical properties of LLDPE can be tuned by manipulating the amount of short-chain branching (SCB) and the short-chain branch distribution (SCBD)<sup>3,4</sup> as well as by controlling the mode of polymerization, catalyst type, pressure, and temperature. Of course, the identity of the comonomer, which inserts the short chain branch into the main chain, is important. Commonly, 1-butene is chosen because of its low cost, but the use of 1-hexene or 1-octene has shown to improve the mechanical properties of the final material.<sup>5</sup> It has also been observed that the properties of LLDPE are affected by interactions between the polymer chains.<sup>6–10</sup>

Commercial LLDPE is usually prepared by chain-growth polymerization using Ziegler–Natta or metallocene chemistry.<sup>11,12</sup> Multisite-initiated Ziegler catalysis favors the insertion of ethylene and produces less well-defined and heterogeneous primary structures and polymers possessing low molecular weights and high molecular weight distributions.<sup>13–15</sup> In contrast, single-site catalysis by metallocene systems produces copolymers with narrower molecular weight distributions and higher comonomer content,<sup>12,16–18</sup> but the problem of working with less well-defined primary structures still remains.

Complete characterization of commercial PE requires detailed study of intra- and intermolecular properties, including molecular weight distribution, chemical composition, sequence length distribution, and long chain branching level. Model systems are often employed because the results can lead to a better understanding of polymer processing and the overall microstructural effects produced by branch perturbations on PE-based materials. In the past, these materials were made by chain-propagation chemistry, which results in the incorporation of unwanted defects via head-to-head or tail-to-tail monomer coupling. The resulting random distribution of alkyl branches along the PE backbone alters the polymer morphology and thermal behavior, thereby precluding effective use as model systems.

The problems associated with chain-growth polymerization can be circumvented by using step-growth condensation polymerization, in particular acyclic diene metathesis (ADMET) polymerization. In this process, the final polymer structure is controlled exclusively by using symmetrical well-defined monomers which undergo solely olefin metathesis to produce PE with precisely known primary structures. The symmetry in the diene monomer is transferred to the polymer repeat unit with nothing lost in terms of structural control. In ADMET, elimination of ethylene gas drives the reaction to yield an unsaturated high molecular weight polymer in the bulk. While chain-growth methods require indirect manipulation of the primary structure,<sup>11</sup> ADMET dictates the final primary structure of the polymer based on the monomer design.<sup>19</sup> The advantage of this approach is the ability to control the polymer architecture by choosing the appropriate monomer building block, thereby circumventing the use of comonomers and monomer feed ratios or the design of specialized catalysts, producing materials that are excellent models to probe ordering of precisely sequenced methylene sequences that resemble ethylene/ $\alpha$ -olefin copolymers.

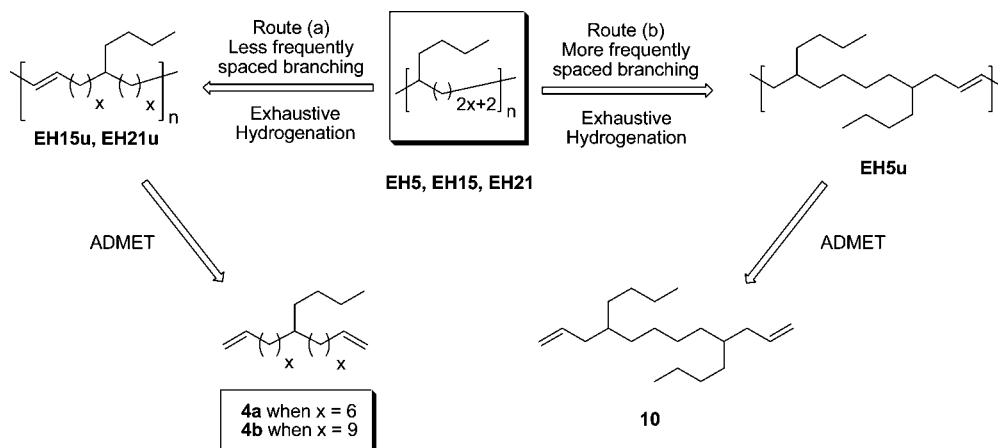
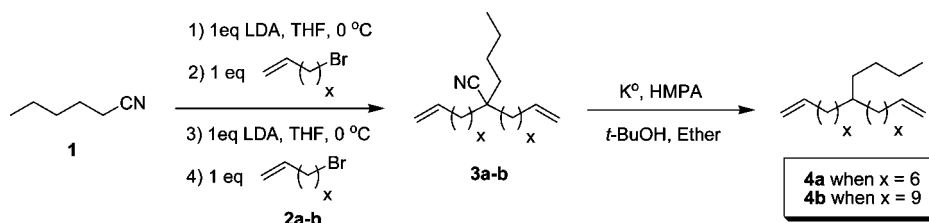
Model PE copolymers can be prepared by ADMET using symmetrically designed  $\alpha,\omega$ -diolefin monomers to produce polymers with well-defined branch identity and distribution along the polymer backbone.<sup>19–25</sup> The polymerization is carried out using Schrock's or first-generation Grubbs catalyst, followed by exhaustive saturation with hydrogen. Scheme 1 shows the retrosynthesis of ADMET copolymers, with butyl branches precisely placed along the polymer backbone.

Initial modeling studies have been performed on PE containing methyl branches on every 9th, 11th, 15th, 19th, and 21st carbon along the backbone.<sup>22</sup> Continuation of this research led to the development of ethyl-branched polyethylene<sup>20</sup> and subsequently to the development of hexyl-branched polyethylene.<sup>21</sup> These polymers have proven to be ideal models of PE copolymers of sequenced ethylene/1-propylene, ethylene/1-butene, and ethylene/1-octene. This paper reports the synthesis, characterization, and thermal behavior of model ethylene/1-hexene copolymers (polyethylene with precisely and irregularly placed butyl branches). The ADMET process was used to produce polyethylene containing butyl branches precisely spaced along the main backbone as well as the irregularly spaced analogues.

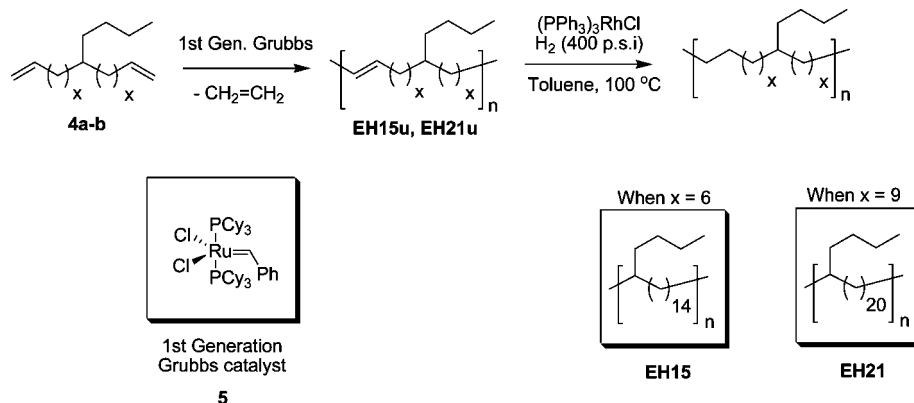
\* Corresponding author. E-mail: wagener@chem.ufl.edu.

<sup>†</sup> Present address: Max Planck Institute for Polymer Research, Mainz, Germany, 55128.

Scheme 1. Retrosynthesis of Precisely Sequenced Ethylene/1-Hexene Copolymers

Scheme 2. Synthesis of  $\alpha,\omega$ -Olefins via Dialkylation/Decyanation of Hexanenitrile

Scheme 3. Synthesis of EH15 and EH21 via ADMET Polymerization–Hydrogenation



## Results and Discussion

**A. Polyethylene Models with Precisely Placed Butyl Branches.** *Monomer Synthesis and ADMET Polymerization of Precisely Sequenced EH Copolymers.* Past attempts to synthesize  $\alpha,\omega$ -diene monomers functionalized only with alkyl branches met with limited success.<sup>20–22</sup> Methodologies were based on the synthesis of the  $\alpha,\omega$ -diene, followed by incorporation of the alkyl branch into the monomeric unit.<sup>20,21</sup> Typically, extension of the alkyl branch was carried out by coupling of carbon moieties mediated via metal complexes, but that strategy resulted in low yields and required many synthetic steps.

Instead of coupling the alkyl branch after formation of the  $\alpha,\omega$ -diene, incorporation of the alkyl branch during formation of the  $\alpha,\omega$ -diene can produce monomers with a variety of branch lengths in high yields with fewer synthetic steps. Nitriles are important precursors in these syntheses because of the reactions that can be performed on the carbon alpha to the nitrile functionality. Double alkenylation of the  $\alpha$ -carbon, followed by the reductive elimination of the nitrile moiety, allows the synthesis of virtually any alkyl  $\alpha,\omega$ -diene. This alkenylation/

decyanation strategy has proven to be useful for the synthesis of a variety of alkyl  $\alpha,\omega$ -dienes with only two synthetic steps in quantitative yields.<sup>26,27</sup>

Scheme 2 illustrates the synthetic methodology to produce  $\alpha,\omega$ -diene monomers **4a** and **4b**, from the alkenylation of hexanenitrile **1** with alkenyl bromides **2a** and **2b**. Alkenylation of **1** in the presence of lithium diisopropyl amide (LDA) and 8-bromooct-1-ene (**2a**) or 11-bromoundec-1-ene (**2b**) produces the cyano  $\alpha,\omega$ -dienes **3a** and **3b** in quantitative yields.<sup>26</sup> Decyanation of nitriles **3a** and **3b** is achieved by transferring one electron from potassium metal to the nitrile group to form a radical anion, which promotes elimination of the cyanide anion. The resulting tertiary radical is further quenched by abstraction of hydrogen from *t*-BuOH to give  $\alpha,\omega$ -diene monomers **4a** and **4b** in quantitative yields.<sup>27</sup> Synthesis of  $\alpha,\omega$ -dienes containing longer runs of methylene units between the terminal olefins is under current investigation.

As shown in Scheme 3, polymerization of  $\alpha,\omega$ -diolefin monomers **4a** and **4b** is carried out with first-generation Grubbs catalyst (**5**) in the absence of solvent. Similar to any step-growth

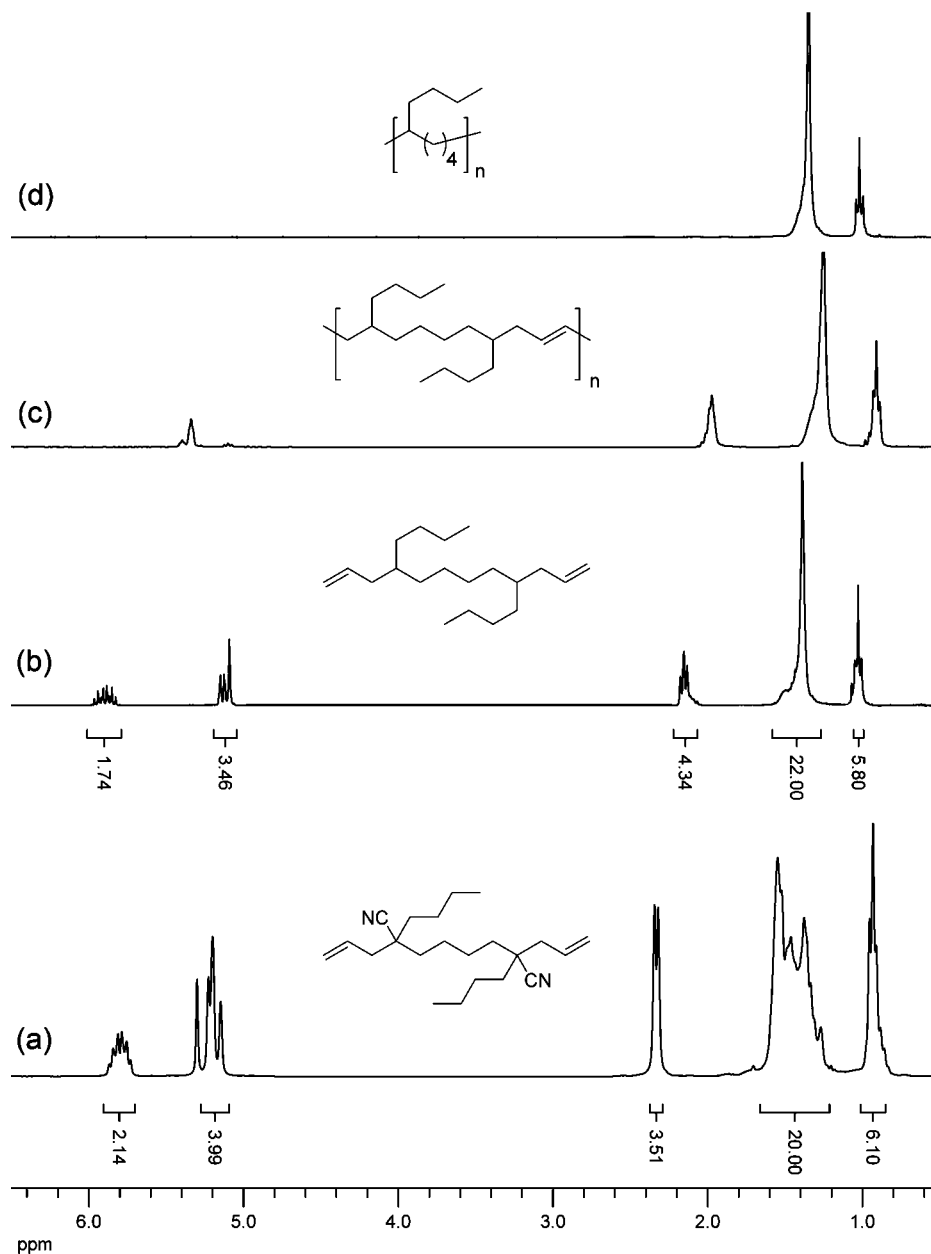


**Figure 1.** Comparison of  $^1\text{H}$  NMR spectra for a typical ADMET polymerization transformation: (a) premonomer **9**, 2,7-diallyl-2,7-dibutyloctanedinitrile; (b) monomer **10**, 5,10-diallyltetradecane; (c) ADMET unsaturated polymer **EH5u**; (d) ADMET saturated polymer **EH5**.

polycondensation, ADMET requires pure monomers to obtain high conversion. The polymerization proceeds efficiently, yielding unsaturated polymers **EH15u** and **EH21u** with less than 1–2% cyclization side reactions. Subsequent exhaustive saturation of the internal olefins with hydrogen gas and Wilkinson catalyst in toluene yields saturated polymers **EH15** and **EH21**. The efficiency of hydrogenation can be followed by the disappearance of the olefin signals in  $^1\text{H}$  NMR (Figure 1) and  $^{13}\text{C}$  NMR (Figure 2) and by the disappearance of the out-of-plane alkene C–H bend using infrared (IR) spectroscopy (Figure 3).

The nomenclature of ADMET products is based on the comonomers for the corresponding copolymer formed by chain addition. All copolymers include the prefix “E” for ethylene, followed by the comonomer type “H” for 1-hexene. Saturation or unsaturation of the main backbone is given by the absence or presence of the suffix “u”, and the branch frequency is indicated by number. For example, **EH21** designates the saturated precisely sequenced ethylene/1-hexene copolymer with a butyl branch on every 21st carbon, while **EH21u** refers to the unsaturated analogue.

Although the synthetic approach described above can be used to prepare EH models containing butyl branches on every 15th and 21st carbon (route (a) in Scheme 1), the synthesis of the monomers for EH copolymer with shorter methylene run lengths between branches has been difficult to accomplish. During the decyanation process (Scheme 2), the intermediate tertiary radical can undergo intraradical cyclization. Unwanted cyclization products were isolated when decyanation chemistry was used to synthesize the  $\alpha,\omega$ -diene monomers containing 3 and 4 methylene groups, 6-butylnon-1,10-diene and 7-butyldodeca-1,2,12-triene.<sup>27</sup> In addition, ADMET polymerization based on 1,6-heptadiene monomers will also result in cyclization by ring-closing metathesis. Therefore, a different approach was used for the synthesis of EH copolymer models possessing butyl branches spaced by fewer than 15 methylene units.

Previous success in the synthesis of EP copolymers containing methyl groups on every 5th and 7th carbon<sup>23</sup> led us to try ADMET polymerization of monomers containing two butyl groups on each monomeric unit. Scheme 4 shows the synthetic approach for obtaining **EH5**, polyethylene containing a butyl

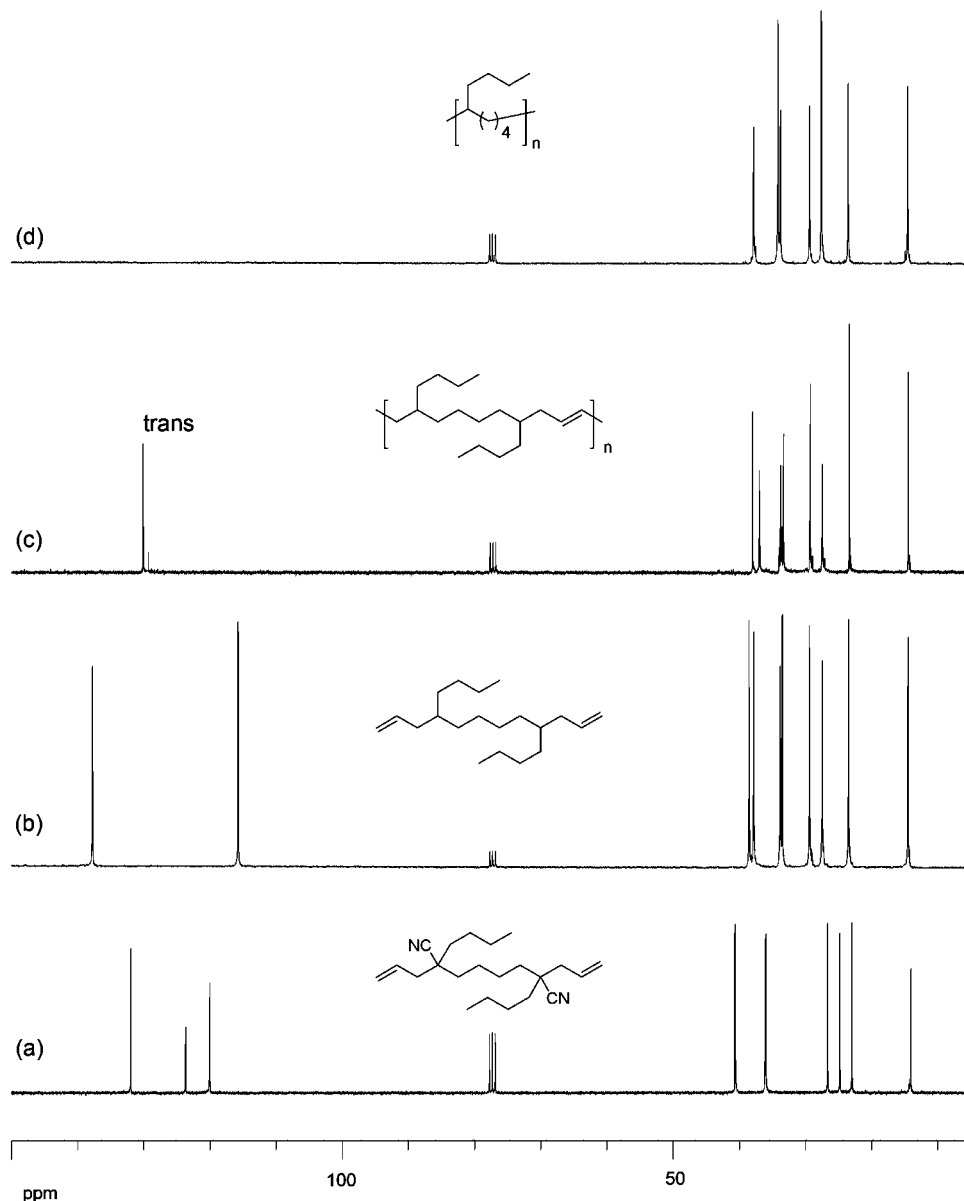


**Figure 2.** Comparison of  $^{13}\text{C}$  NMR spectra for a typical ADMET polymerization transformation: (a) premonomer **9**, 2,7-diallyl-2,7-dibutyloctanedinitrile; (b) monomer **10**, 5,10-diallyltetradecane; (c) ADMET unsaturated polymer **EH5u**; (d) ADMET saturated polymer **EH5**.

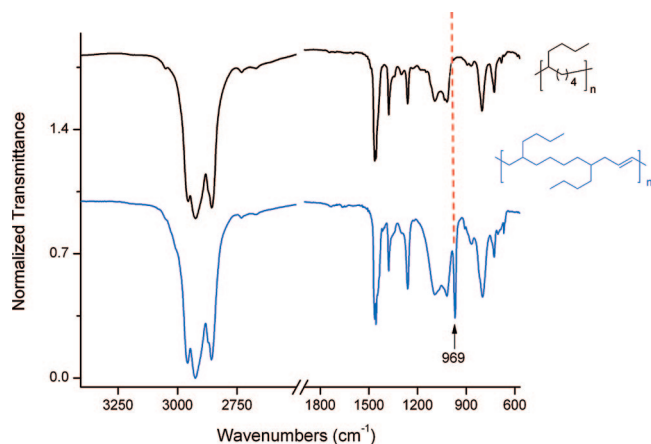


**Figure 3.** Infrared spectra for the ADMET unsaturated and saturated polymers **EH5u** (bottom) and **EH5** (top).

branch on every 5th carbon. Monoalkenylation of hexanenitrile **1** with allyl bromide **6** in the presence of LDA yields nitrile **7**.

Disubstitution of 1,4-dibromobutane quantitatively yields 2,7-diallyl-2,7-dibutyloctanedinitrile **9**, which undergoes decyanation to produce 5,10-diallyltetradecane (monomer **10**). Polymerization of **10** in presence of first-generation Grubbs catalyst proceeds smoothly to produce unsaturated polymer **EH5u**. Exhaustive hydrogenation of the unsaturated polymer in the presence of *p*-toluenesulfonyl hydrazide, tripropylamine, and xylene yields **EH5**. This methodology allows the synthesis of highly branched sequenced linear low-density ethylene/1-hexene copolymers. The correct design of the monomeric unit circumvents ring-closing metathesis, which is usually observed in structures based on 1,6-heptadiene.

Regardless of the strategy employed for the  $\alpha,\omega$ -diene monomer preparation, high molecular weight polymers were afforded via ADMET for both monoalkyl (**4a** and **4b**) and dialkyl  $\alpha,\omega$ -diolefins (**10**). Table 1 shows the molecular weights for the precisely sequenced ethylene/1-hexene copolymer models obtained via ADMET polymerization. The weight-average molecular weights were obtained by gel permeation chromatography (GPC) versus polystyrene standards. The small difference in molecular weight before and after hydrogenation



Scheme 4. Synthesis of EH5 via ADMET Polymerization–Hydrogenation

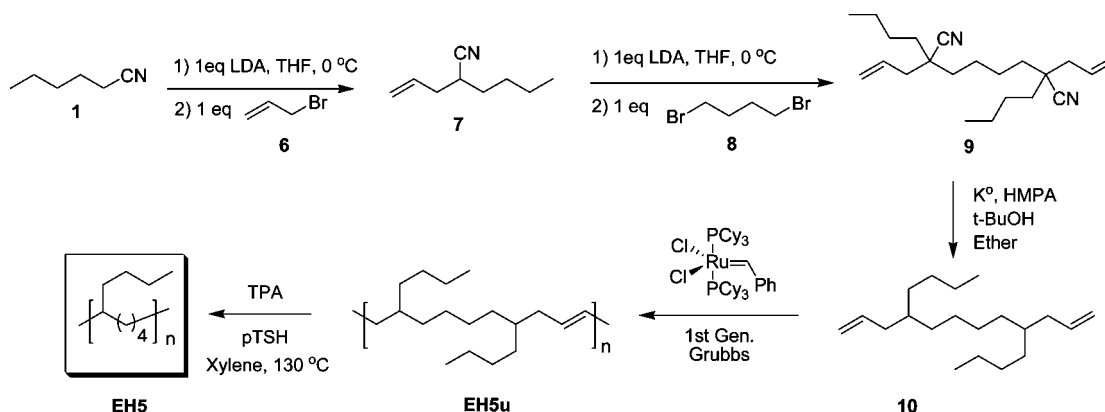


Table 1. Molecular Weights and Thermal Data for ADMET Models, EH Precisely Sequenced Copolymers

model EH copolymer	butyl on every <i>n</i> th backbone carbon <i>n</i> <sup>a</sup>	butyl branch content per 1000 carbons	$\overline{M}_w \times 10^3$ (PDI) <sup>c</sup>		<i>T</i> <sub>m</sub> (°C) (peak)	$\Delta h_m$ (J/g)
			unsaturated <sup>b</sup>	saturated <sup>b</sup>		
<b>EH5</b>	5	200	21.2 (1.7)	20.8 (1.8)	amorphous	
<b>EH15</b>	15	67	47.6 (1.9)	48.1 (1.9)	−33, −53	13
<b>EH21</b>	21	48	41.5 (1.8)	40.3 (1.7)	14	47

<sup>a</sup> Branch content based on the hydrogenated repeat unit. <sup>b</sup> Weight-average molecular weight data obtained using GPC in THF (40 °C) relative to polystyrene standards (g/mol). <sup>c</sup> PDI, polydispersity index ( $\overline{M}_w/\overline{M}_n$ ).

suggests that the main PE chains are not affected by the saturation process. As shown previously by Smith et al., the range of molecular weights observed for our model materials (20 000–40 000 g/mol by GPC) is sufficient to model the thermal behavior of industrially produced EH copolymers.<sup>22</sup>

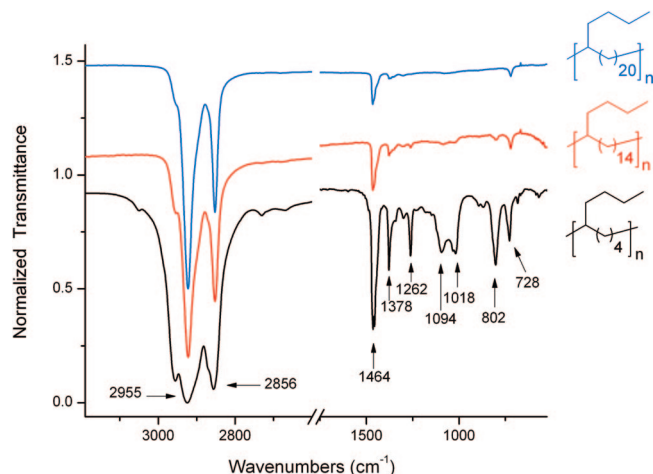
**Structural Data for Precisely Sequenced EH Copolymers.** Control over the polymer primary structure by ADMET makes it possible to obtain information about the macromolecular structure of linear low-density polyethylene having “defects” intentionally and evenly placed along the main chain. Examination of <sup>1</sup>H and <sup>13</sup>C NMR spectra of monomers and polymers indicates complete transformation and control over the primary structure. Figure 1 shows the <sup>1</sup>H NMR spectra for the ADMET polymer **EH5** and its precursors. The transformation begins with the decyanation of 2,7-diallyl-2,7-dibutyloctanedinitrile (**9**), yielding 5,10-diallyltetradecane monomer (**10**), shown in Figure 1a,b. Polymerization of **10** yields the unsaturated polymer **EH5u**. Analysis of the olefin region (5–6 ppm) supports the fact that the polymer is formed from a single repeat unit, which is evidenced by the disappearance of the terminal olefin signals (5.1 and 5.9 ppm in Figure 1b) and the formation of the internal olefin (5.3 ppm in Figure 1c). Further hydrogenation of the internal olefins yields **EH5**, a precisely sequenced ethylene/1-hexene copolymer, which shows no observable traces of olefin by <sup>1</sup>H NMR (Figure 1d).

Figure 2 shows the <sup>13</sup>C NMR spectra for the same compounds. In the spectrum for the 2,7-diallyl-2,7-dibutyloctanedinitrile (**9**, Figure 2a), the singlets at 120.1 and 132.0 ppm show the presence of terminal olefins, and the signal at 123.7 ppm corresponds to the nitrile carbon. Absence of the signal at 123.7 ppm after decyanation (Figure 2b) demonstrates complete elimination of the CN group. On the basis of the values of the chemical shifts for the singlets corresponding to the terminal olefin (120.1 and 132.0 ppm in premonomer **9** versus 115.8 and 137.8 ppm in monomer **10**) and the data obtained from <sup>1</sup>H NMR, it can be concluded that the change in chemical shifts is due solely to the absence of the nitrile functionality and not to isomerization of the terminal olefin to an internal olefin. ADMET polymerization of **10** yields the unsaturated polymer **EH5u**. Comparison of parts b and c of Figure 2 shows the disappearance of the signals belonging to the terminal olefin at

115.8 and 137.8 ppm and formation of the new internal olefin (cis at 129.4 ppm and trans at 130.1 ppm) produced from the effective metathesis polymerization. Subsequent hydrogenation of the internal olefin yields the saturated polymer **EH5**, whose <sup>13</sup>C NMR spectrum (Figure 2d) shows no detectable trace of olefins. Upon close inspection of the <sup>13</sup>C NMR data during the transformation, it can be concluded that the ADMET polymer **EH5** is formed only by symmetrical repeating units, in which the methyl from the pendant side chain butyl branch resonates at 14.5 ppm (−CH<sub>3</sub>), the methylene alpha to the terminal methyl group at 23.6 ppm (−CH<sub>2</sub>CH<sub>3</sub>), and the carbon at the branch point at 37.8 ppm.

Further studies of these precisely sequenced ethylene/1-hexene copolymer models were performed using infrared (IR) spectroscopy. Although <sup>1</sup>H and <sup>13</sup>C NMR showed no detectable remaining traces of olefins after exhaustive hydrogenation, IR spectroscopy also offers a sensitive method to observe whether complete saturation has occurred.<sup>19,24,25</sup> Figure 3 shows the IR spectra before and after exhaustive hydrogenation of the model material. The unsaturated material **EH5u** (Figure 3, bottom curve) shows an absorption band at 969 cm<sup>−1</sup> due to the out-of-plane C–H bend in the alkene, which disappears after complete hydrogenation to **EH5** (Figure 3, top curve).

In the past, Tashiro et al. carried out a structural investigation for polyethylene crystals using complementary data from wide-angle X-ray diffraction (WAXD), IR, and Raman spectroscopy.<sup>28</sup> They concluded that the scissoring at 1466 cm<sup>−1</sup> and methylene rock at 721 cm<sup>−1</sup> indicate a hexagonal crystal structure, while the double methylene rock at 719 and 730 cm<sup>−1</sup> and single band at 1471 cm<sup>−1</sup> correspond to an orthorhombic crystal structure. Similar IR studies and WAXD measurements showed the same connections of interchain defects to crystal behavior and crystal packing for ADMET PE containing methyl branches randomly placed along the backbone.<sup>29</sup> Although the low melting transitions of our semicrystalline EH model copolymers made difficult to obtain solid-state data, and the information collected from film casting cannot be directly related to crystallographic arrangements, detailed IR analysis for the synthesized **EH** copolymers gives an idea of their behavior at room temperature.



**Figure 4.** Infrared spectra for the ADMET saturated polymers **EH5** (bottom), **EH15** (center), and **EH21** (top).

The IR spectra for **EH5**, **EH15**, and **EH21** in Figure 4 are dominated by two sets of absorption bands (2900 and 1464  $\text{cm}^{-1}$ ), which are usually observed when the packing is disorganized. While orthorhombic crystals show the characteristic Davidov splitting at 720  $\text{cm}^{-1}$  due to the methylene rocking,<sup>30,31</sup> our EH models display a single rocking absorbance at 728  $\text{cm}^{-1}$ , indicating the absence of orthorhombic crystal behavior. Moreover, the two experimental absorption bands at 728 and 1464  $\text{cm}^{-1}$  are characteristic of a highly disordered phase, similar to the pattern observed in previous studies containing precisely spaced methyl,<sup>22</sup> ethyl,<sup>20</sup> and hexyl branches.<sup>21</sup> Similar to PE models possessing hexyl branches, EH models display characteristic bands at 2955, 1464, and 728  $\text{cm}^{-1}$ , which suggest that the larger defect volume imparted by evenly spaced butyl branches does not alter the methylene scissoring and wagging regions.

The IR data presented above indicate that the precisely sequenced model copolymers **EH5**, **EH15**, and **EH21** contain high defect concentrations. Although we cannot rule out the presence of hexagonal crystals, the absence of the characteristic orthorhombic signature is clear in the IR spectra. In order to understand how the crystal packing occurs and also how the crystal grow behavior and nucleation is in our EH models, a series of solid-state NMR experiments and subambient X-ray diffraction experiments (SAXS and WAXD) are currently underway.

**Thermal Behavior for Precisely Sequenced EH Copolymers.** Numerous reports are available concerning the structure and thermal properties of branched PE, particularly for LLDPE and HDPE made by chain-addition chemistry.<sup>7–9,32–35</sup> Although the ultimate goal has been to understand the relationship between structure and physical properties, many previous investigations attempted to correlate initial monomer feed ratios to the final properties of the produced materials. A major drawback to this approach is the problem of imperfect primary structures, which are always present in materials produced by chain-addition chemistry. In contrast, our well-defined primary structures permit studies of the thermal properties of precisely sequenced ethylene/1-hexene copolymers.

Figure 5 shows the DSC curves for **EH5**, **EH15**, and **EH21**, and the physical data are summarized in Table 1. Similar to previous studies involving regularly spaced methyl (EP),<sup>22</sup> ethyl (EB),<sup>20</sup> and hexyl branches (EO),<sup>21</sup> the precisely sequenced ethylene/1-hexene (EH) copolymers display sharp endothermic transitions, with none of the broadening observed for copolymers obtained via chain polymerization.<sup>7–9,32–35</sup> The data in Table 1 show that the EH models follow the trend previously observed

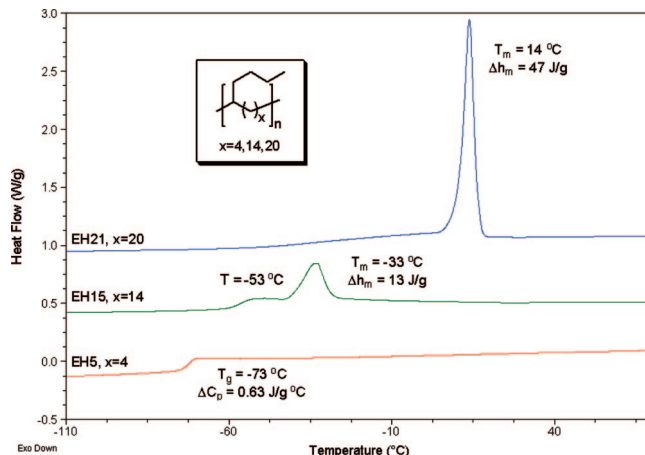


**Figure 5.** DSC profile for ADMET polymers: **EH5** (bottom), **EH15** (center), and **EH21** (top).

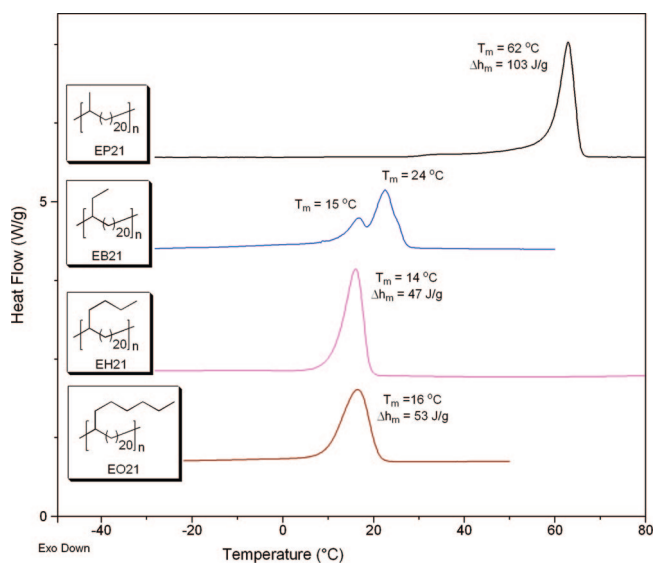


**Figure 6.** DSC profiles for ADMET polymers possessing alkyl branches on every 21st carbon. Data for **EP21**, **EB21**, and **EO21** taken from Wagener et al.<sup>20–22</sup>

for EP, EB, and EO model copolymers, for which melting temperature, heat of fusion, and degree of crystallinity all decrease as the percentage of 1-olefin increases. The **EH21** and **EH15** copolymers are both semicrystalline materials, with percent crystallinity decreasing as the branch content increases. When the branch content increases to 200 branches per 1000 backbone carbons (**EH5**), a fully amorphous material is produced. The observation of two endotherms for **EH15** is being further investigated by modulated DSC.

The DSC profiles for a series of precisely sequenced copolymers containing alkyl branches on every 21st carbon (Figure 6) show an obvious correlation between branch size and thermal behavior. While **EP21** exhibits a sharp melting point at 62 °C, one-carbon homologation on the side branch (**EB21**) produces a 40 °C lower bimodal melting transition at 24 °C (major peak) and 15 °C (minor peak). This bimodal behavior could be produced by many factors; for example, the presence of a premelting endotherm due to the existence of two distinct arrays packing differently in the crystal structure. Increasing the branch size from two to four carbons (**EH21**) produces a sharp endotherm at 14 °C, observed at the same temperature as the small endotherm for **EB21**. This indicates that **EH21** contains only one packing array, which is different from that observed for **EP21**. Interestingly, addition of two more carbons



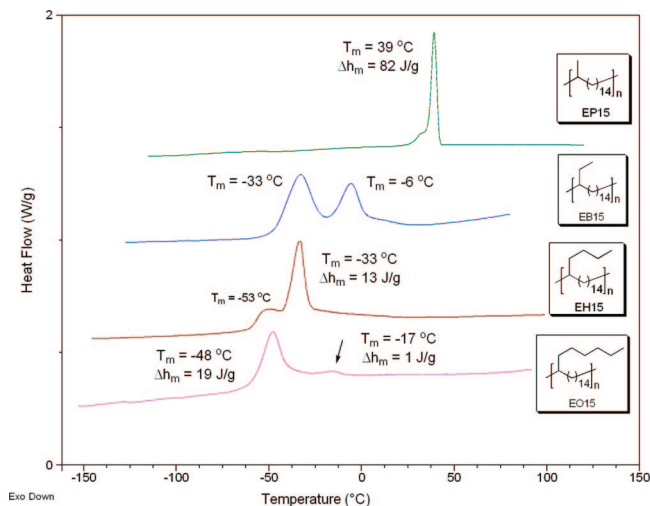


**Figure 7.** DSC profiles for ADMET polymers possessing alkyl branches on every 15th carbon. Data for **EP15**, **EB15**, and **EO15** taken from Wagener et al.<sup>20–22</sup>

to the side branch (**EO21**) seems to have no effect on the thermal behavior, suggesting that **EH21** and **EO21** are quite similar in nature.

The same trends are observed when the branch spacing is 14 methylene units, as shown in Figure 7. Incorporation of a methyl “defect” on every 15th carbon (**EP15**) renders a material with a sharp endotherm with a peak melting of 39 °C. When the side chain is extended to two carbons (**EB15**), a bimodal transition is observed. In contrast to the behavior of **EB21**, the smaller fraction corresponds to the higher melting component (−6 °C, minor fraction, vs −33 °C, major fraction). As in the case of **EB21** and **EH21**, the larger overall heat flow observed for **EH15** corresponds to the lower temperature endotherm for **EB15**, but there is an additional small contribution at −53 °C. The peak at −53 °C for **EH15** overlaps the endotherm previously reported for **EO15** at −48 °C, but the latter also shows a small peak at −17 °C. When the branch distance is maintained constant, whether 20 carbons (Figure 6) or 14 carbons apart from each other (Figure 7), a clear depression of the melting point of the model materials is observed when the branch size is gradually increased from one carbon unit (EP models) to six carbon units (EO models). Although EO and EH copolymers made via chain-growth chemistry are amorphous due to their high comonomer content (13–14%), precisely sequenced ethylene/1-olefin models containing an alkyl branch on every 21st and 15th carbon contain more organized primary structures and are semicrystalline materials.

When the “defects” are evenly and precisely distributed along the polyethylene main chain, the well-organized primary structures permit the formation of semicrystalline materials. However, regardless of the branch identity or the order imparted by the precisely sequenced comonomer incorporation, the ability to form semicrystalline materials is lost if the “defect” becomes more frequent along the polyethylene backbone, as shown in Figure 8. The DSC’s of both **EP5** and **EH5** model copolymers indicate that these compounds are fully amorphous materials. It is noteworthy that the presence of the bulkier butyl branch on **EH5** causes the glass transition previously observed for **EP5** at −65 °C to decrease to −73 °C, as is expected.

**B. Polyethylene Models with Irregularly Placed Butyl Branches.** The first part of this paper has described the ADMET synthesis of polyethylene with precisely spaced butyl branches. While these are not models for the industrial LLDPE in the true sense of the word, they represent an excellent starting point for the study of structure/property relationships in ethylene-based

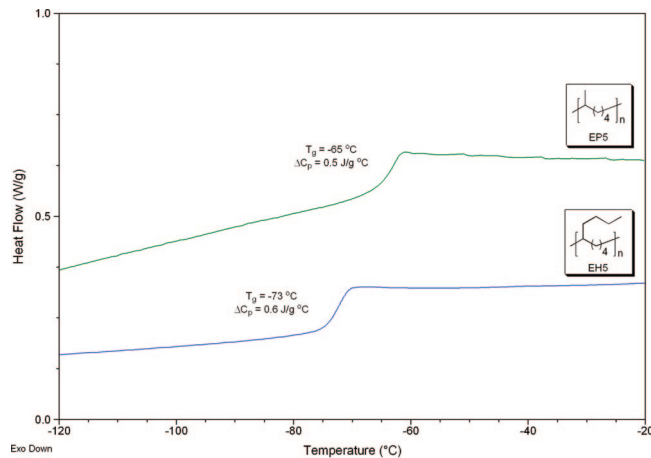


**Figure 8.** DSC profiles for ADMET polymers possessing alkyl branches on every 5th carbon. Data for **EP5** taken from Baughman, Sworen, and Wagener.<sup>23</sup>

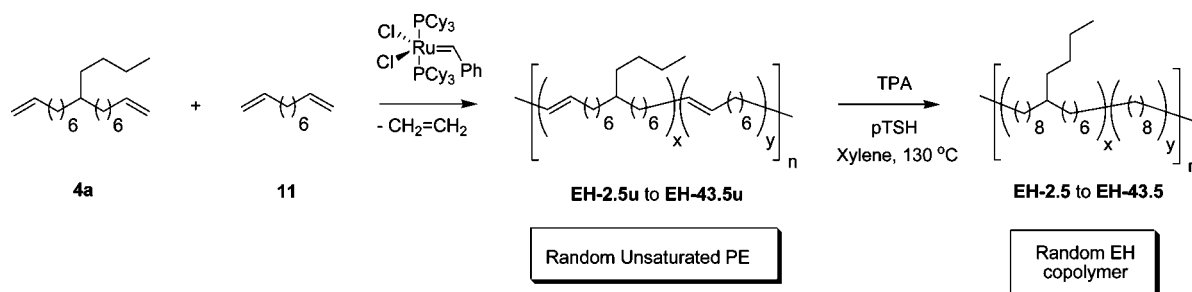
materials because they allow the effects of specific structural features to be isolated and investigated. As described above, DSC results show that these well-organized primary structures display unique thermal behavior.

In contrast, because of inevitable chain transfer or chain walking, industrially prepared LLDPE made by copolymerization of ethylene with  $\alpha$ -olefins produces structures with alkyl branches of varying lengths randomly spaced along the main chain. Thus, realistic models of commercial ethylene/1-alkene copolymers should have branches of known chain length, but with random spacing. These materials can also be synthesized by the ADMET process, as demonstrated previously for EP copolymers and halogen-substituted polyethylene.<sup>29,36</sup>

**Monomer Synthesis and ADMET Polymerization of Irregularly Sequenced EH Copolymers.** Using metathesis chemistry for modeling PE structures, the branch frequency can be controlled by copolymerization of monomeric units with the correct architecture. Because the comonomers have similar reactivities, total conversion of the monomers into copolymer permits manipulation of the branch content of the final material. For example, ADMET copolymerization of a monomer containing the required branch identity (butyl branch) along with 1,9-decadiene produces an irregularly sequenced ethylene/1-hexene copolymer. In chain-growth chemistry the branch content is directly related to both the molar and reactivity ratios, but step-growth chemistry permits manipulation of the branch content of the final material by controlling only the initial molar ratio of the two monomers without dealing with reactivity ratios.

As shown in Scheme 5, ADMET copolymerization of 9-butylheptadeca-1,16-diene (**4a**) with 1,9-decadiene (**11**) in the presence of first-generation Grubbs catalyst yields unsaturated polymers **EH-2.5u** to **EH-43.5u**. Exhaustive hydrogenation of the unsaturated polymers using *p*-toluenesulfonyl hydrazide, tripropylamine, and xylene yields irregularly sequenced ethylene/1-hexene copolymers **EH-2.5** to **EH-43.5**. The nomenclature for the unsaturated/saturated polymers is based on the comonomer content. The prefix “E” denotes polyethylene, followed by the comonomer type “H” for 1-hexene. Saturation or unsaturation of the main backbone is given by the absence or presence of the suffix “u”. The branch content is given by number; e.g., **EH-2.5** designates the saturated irregularly sequenced ethylene/1-hexene copolymer, which contains 2.5 butyl branches per 1000 backbone carbons, while **EH-2.5u** refers to its unsaturated analogue.

Copolymerization of different molar ratios of **4a** and **11** yields a series of materials with varying butyl branch content, as shown in Table 2. The lower limit of comonomer content incorporation

**Scheme 5. Synthesis of EH Random Materials by ADMET Copolymerization of 9-Butylheptadeca-1,16-diene (4a) and 1,9-Decadiene (11)****Table 2. Molecular Weights for Unsaturated and Saturated EH Irregularly Sequenced Copolymers Prepared by ADMET**

copolymer with irregularly placed butyl branches	butyl branch content per 1000 backbone carbons <sup>a</sup>	9-butyl-heptadeca-1,16-diene ( <b>4a</b> ), mol %	1,9-decadiene ( <b>11</b> ), mol %	$\bar{M}_w \times 10^3$ (PDI) <sup>c</sup>	
				unsaturated <sup>b</sup>	saturated <sup>b</sup>
<b>EH0</b>	0.0	0	100	42.5 (1.8)	44.9 (1.8)
<b>EH-2.5</b>	2.5	2	98	40.1 (1.7)	39.8 (1.8)
<b>EH-6.0</b>	6.0	5	95	39.5 (1.7)	40.7 (1.6)
<b>EH-11.5</b>	11.5	10	90	38.7 (1.6)	37.8 (1.8)
<b>EH-21.3</b>	21.3	20	80	48.4 (1.6)	45.1 (1.6)
<b>EH-37.0</b>	37.0	40	60	37.5 (1.8)	38.1 (1.7)
<b>EH-43.5</b>	43.5	50	50	38.4 (1.8)	37.3 (1.8)
<b>EH15</b>	66.7	100	0	47.6 (1.9)	48.1 (1.9)

<sup>a</sup> Determined by an average of both the <sup>1</sup>H NMR (300 MHz) and <sup>13</sup>C NMR (125 MHz) data. <sup>b</sup> Weight-average molecular weight data obtained by GPC in THF (40 °C) relative to polystyrene standards (g/mol). <sup>c</sup> PDI, polydispersity index ( $\bar{M}_w/\bar{M}_n$ ).

is set by linear PE made by homopolymerization of **11**, which yields linear polyethylene with no alkyl branches **EH0**.<sup>19</sup> Incorporation of 2 mol % of **4a** renders **EH-2.5u**, which has  $\bar{M}_w = 40\,000$  g/mol and a polydispersity index (PDI) of 1.7 via GPC versus polystyrene standards. Subsequent saturation yields **EH-2.5** with a  $\bar{M}_w = 39\,800$  g/mol and PDI = 1.8. The small change in molecular weight after saturation suggests that the main chain is not affected by the hydrogenation process. Weight-average molecular weights of materials with higher comonomer content, from **EH-6.0** to **EH-43.5**, are also listed on Table 2. Incorporation of 5, 10, 20, 40, and 50 mol % of comonomer **4a** yields materials containing 6.0, 11.5, 21.3, 37.0, and 43.5 butyl branches per 1000 backbone carbons, respectively. The models in Table 2 have weight-average molecular weights ranging from 37 000 to 45 000 g/mol by GPC. Regardless of the molecular weight determination method, the molecular weights displayed in Table 2 for our irregularly sequenced ethylene/1-hexene copolymers are sufficiently high to serve as models for EH copolymers. However, it is noteworthy that this model limits the branch to branch distance to at least 13 methylene units, and sequences with higher branch content, for example EHH or HEH sequences, are not obtained with this approach.

#### Structural Data for Irregularly Sequenced EH Copolymers.

The butyl branch content initially determined by the molar content of monomer **4a** was verified for the final materials, **EH-2.5** to **EH-43.5**, by a combination of <sup>1</sup>H and <sup>13</sup>C NMR spectroscopy, as previously reported by Wagener et al. for ethylene/propene copolymers.<sup>29</sup> The butyl branch contents calculated using both the <sup>1</sup>H and <sup>13</sup>C data are given in Table 2.

Figure 9a shows the <sup>13</sup>C NMR spectrum for the homopolymerization of 1,9-decadiene after exhaustive hydrogenation (**EH0**). The linear polyethylene presents a dominant signal at  $\delta$  29.99 ppm (signal E), which corresponds to the methylene units forming the polyethylene main chain. Detailed <sup>13</sup>C NMR analysis allows visualization of signals A ( $\delta$  14.31 ppm), B ( $\delta$  22.94 ppm), C ( $\delta$  32.22 ppm), and D ( $\delta$  29.60 ppm), which correspond to the end groups of the terminal polyethylene chain, as shown in Figure 9a. In-depth <sup>13</sup>C NMR analysis for the perfectly sequenced **EH15** copolymer permits the visualization

of the carbon at the branch point at  $\delta$  37.62 ppm (signal V), as shown in Figure 9c. Similar to the spectrum shown in Figure 9a, the <sup>13</sup>C NMR for **EH15** (Figure 9c) is dominated by the signal at  $\delta$  29.99 ppm corresponding to the PE backbone. Close inspection of spectra c and a of Figure 9 shows that the terminal  $-\text{CH}_2\text{CH}_2\text{CH}_3$  linkage (A, B, and C) is present in both, indicating that the presence of butyl branches precisely placed on every 15th carbon affects carbons no greater than three positions from an individual branch located on the polymer backbone. The same effect was observed by Wagener et al. during <sup>13</sup>C NMR experiments of polyethylene containing methyl branches.<sup>29</sup> Moreover, the spectrum in Figure 9c shows the resonances belonging to the butyl branch, I ( $\delta$  14.39 ppm), II ( $\delta$  23.40 ppm), III ( $\delta$  30.40 ppm), and IV ( $\delta$  33.63 ppm), and the three carbons on the main chain around the branch point, VI ( $\delta$  33.95 ppm), VII ( $\delta$  26.95 ppm), and VIII ( $\delta$  29.20 ppm). Figure 9b shows the <sup>13</sup>C NMR spectrum for the irregularly sequenced ethylene/1-hexene model copolymer containing 43.5 butyl branches per 1000 backbone carbons (**EH-43.5**). Like the spectra in Figure 9a,c, the spectrum in Figure 9b is dominated by the signal at  $\delta$  29.99 ppm corresponding to the PE backbone. Detailed analysis of the resonances observed for **EH-43.5** indicates that both **EH0** and **EH15** characteristics are present; the terminal end groups (A, B, and C) are present as well as the resonances corresponding to the butyl branch (I, II, III, and IV). The main differences between the spectra in Figure 9b,c are the relative areas for the signals corresponding to the butyl branch (signals I, II, III, and IV), which are all smaller for **EH-43.5** (43.5 butyl branches per 1000 backbone carbons, Figure 9b), compared to **EH5** (200 butyl branches per 1000 backbone carbons Figure 9c).

In addition to the NMR characterization of the irregularly sequenced ethylene/1-hexene ADMET copolymers, infrared (IR) spectroscopy was used to study EH copolymers **EH-2.5** to **EH-43.5**. Although X-ray diffraction techniques provide the absolute crystal structure, IR spectroscopy can give an idea of the order or crystal structure for these model polymers. Pracella et al. reported the structural characterization of EH copolymers made via chain-growth chemistry.<sup>30</sup> In their report, detailed IR study for EH copolymers facilitated the determination of the comono-

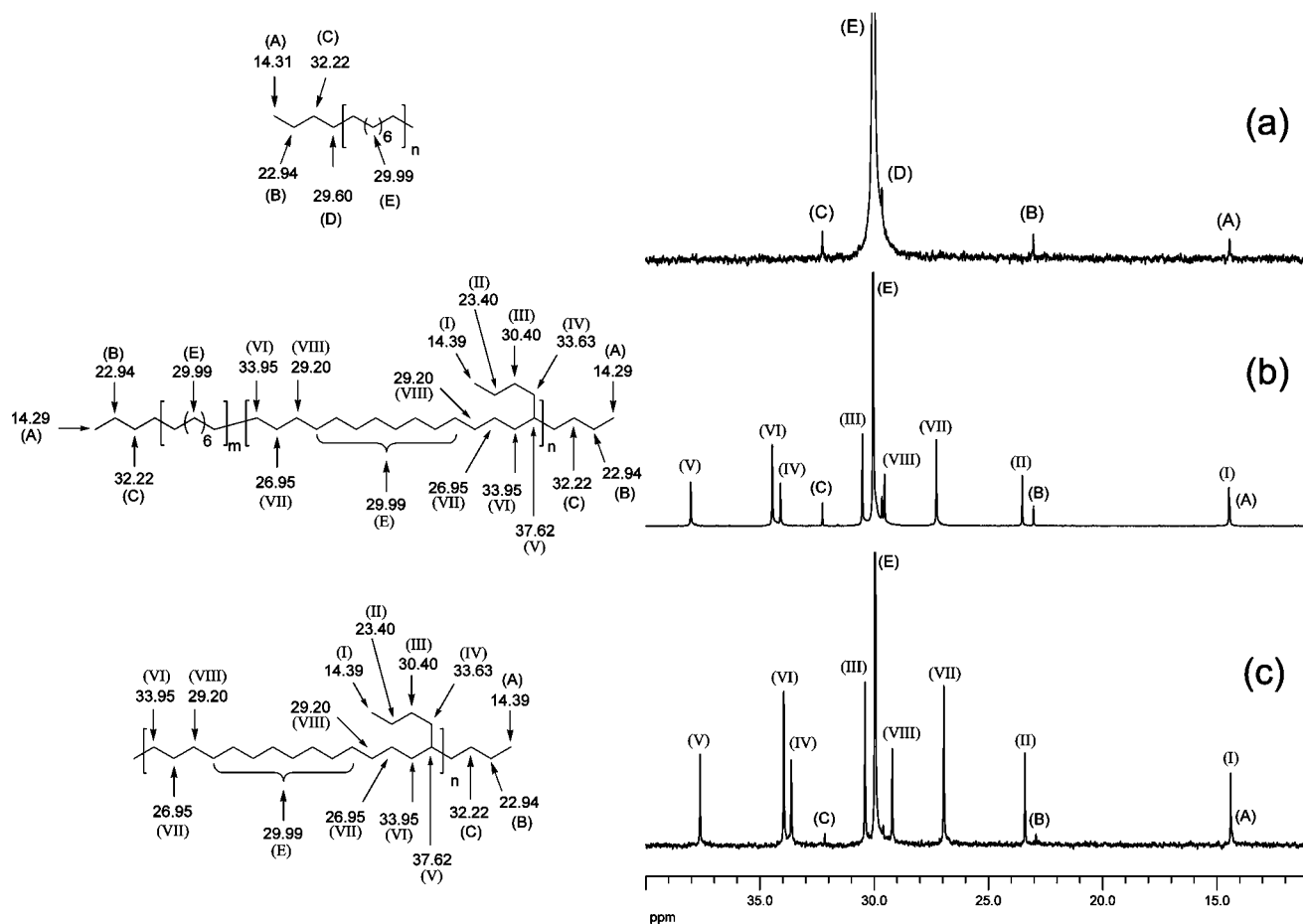


**Figure 9.** Comparison of  $^{13}\text{C}$  NMR spectra for (a) linear ADMET PE **EH0**, (b) irregularly sequenced **EH-43.5** ADMET polymer, and (c) precisely sequenced **EH15** ADMET polymer.

mer contents in the 1–5 mol % range. Led by Pracella's finding, we have focused the IR analysis on three main regions: 1490–1440, 1400–1330, and 750–690  $\text{cm}^{-1}$ .

The region from 1400 to 1330  $\text{cm}^{-1}$  is useful for compositional analysis of ethylene/ $\alpha$ -olefin copolymers. In this region (Figure 10a), linear polyethylene **EH0** shows a broad absorption band at 1369  $\text{cm}^{-1}$  corresponding to the methylene wagging.<sup>30,37</sup> Incorporation of butyl branches along the PE backbone results in formation of a new absorption band at 1378  $\text{cm}^{-1}$ , corresponding to the symmetric deformation of the terminal methyl on the butyl branch. While the band at 1378  $\text{cm}^{-1}$  is very weak for **EH-2.5** due to the low comonomer content, materials with higher comonomer contents present more intense bands with areas proportional to the branch content.

Figure 10b shows spectra of the 1490–1440  $\text{cm}^{-1}$  region, which contains bands at 1473 and 1463  $\text{cm}^{-1}$  due to the bending of methylene units in the crystalline and amorphous phases. Linear ADMET polyethylene **EH0** shows two bands at 1473 and 1463  $\text{cm}^{-1}$ , suggesting the presence of a well-organized highly crystalline structure. However, gradual incorporation of butyl branches decreases the areas of both bands, indicating a reduction in the degree of crystallinity because of the formation of less organized structures in the polymers with high butyl branch content.

While the precisely sequenced EH model copolymers, **EH5**, **EH15**, and **EH21** showed no signs of orthorhombic crystal behavior (Figure 4), usually observed as a Davydov splitting at 719 and 730  $\text{cm}^{-1}$  due to the methylene rocking, the irregularly sequenced EH model copolymers show the characteristic pattern of an orthorhombic lattice (Figure 10c).<sup>30,38</sup> It is important to note that the characteristic bands suggesting the orthorhombic

crystal behavior are most pronounced in the linear ADMET polyethylene possessing no branches (**EH0**). Increasing the comonomer content causes the intensities of the absorption bands at 719 and 730  $\text{cm}^{-1}$  to decrease. In order to clarify how the crystallization process occurs in our irregularly sequenced EH model copolymers, a series of solid-state NMR, SAXS, and WAXD experiments are currently under study.

**Thermal Behavior of Irregularly Sequenced EH Copolymers.** While numerous investigations are available concerning the structure and thermal properties of ethylene/1-hexene copolymers made via chain chemistry, the new ADMET copolymers have the proper primary structures needed to gain an understanding of the relationship between comonomer content and thermal behavior. The first attempt in modeling irregularly placed alkyl branches prepared by ADMET chemistry was carried out using ethylene/propene (EP) copolymers.<sup>29</sup> Although sharp endotherms were observed for EP random models containing up to 25 methyl branches per 1000 backbone carbons, broad endotherms were observed for EP random models with 43 methyl branches per 1000 backbone carbons ( $\sim 10$  mol % of propylene). The same effect has been observed for EP random copolymers made via Ziegler–Natta chemistry with comonomer content greater than 15 mol %.

Similar to ADMET EP random model copolymers, the ADMET EH model copolymers give sharp endotherms at lower comonomer content, as shown in Figure 11. Linear polyethylene without branches (**EH0**) has the highest melting temperature ( $T_m = 130$  °C) and heat of fusion ( $\Delta h_m = 205$  J/g). Incorporation of small amounts of butyl branches irregularly placed along the PE backbone has only a small effect on the melting temperature of the material. For example, incorporation of 2.5 (**EH-2.5**) and



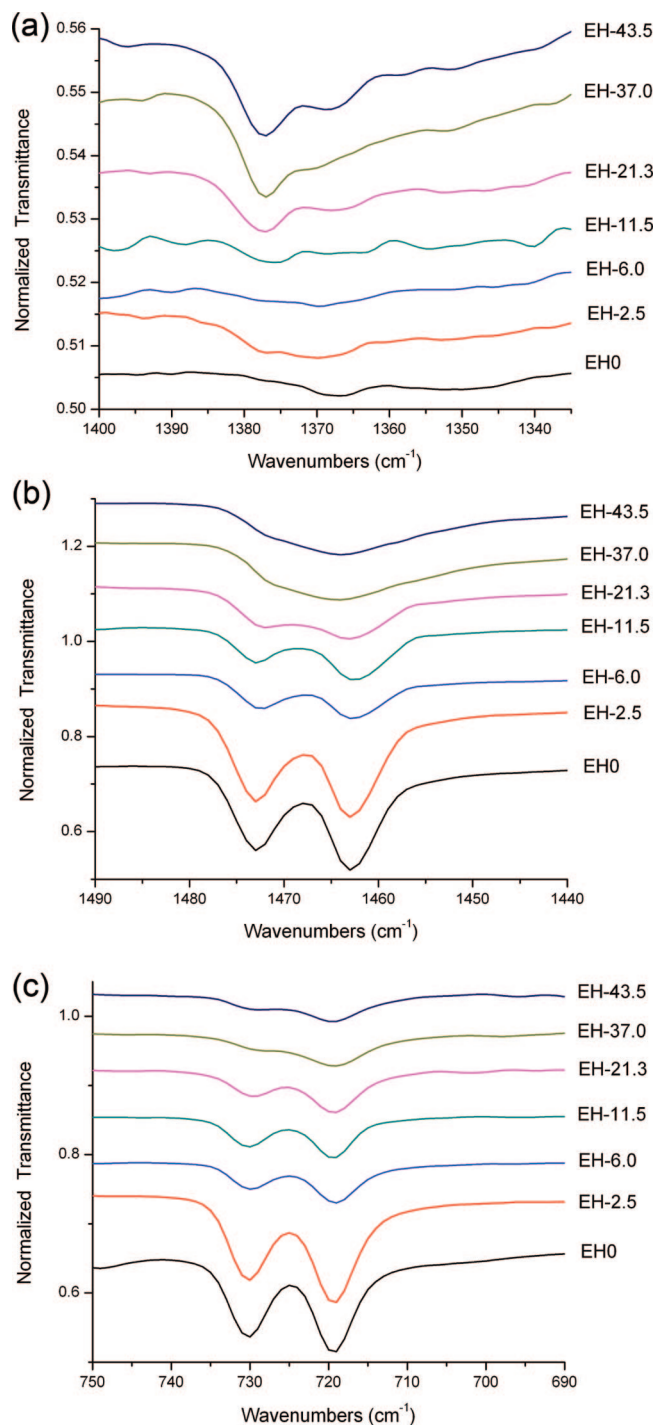


**Figure 10.** Infrared spectra for the irregularly spaced ADMET copolymers **EH0**–**EH43.5**: (a) recorded in the region of 1400–1335  $\text{cm}^{-1}$ , (b) recorded in the region of 1490–1440  $\text{cm}^{-1}$ , and (c) recorded in the region of 750–690  $\text{cm}^{-1}$ .

6 butyl branches (**EH-6.0**) per 1000 backbone carbons reduces the melting temperature to 126 and 122  $^{\circ}\text{C}$ , respectively. In contrast, the enthalpies of fusion of such materials decrease significantly, by 12 J/g for **EH-2.5** and 76 J/g for **EH-6.0**. This effect can be attributed to the decrease in crystallinity when larger numbers of butyl branches are incorporated.

Similar to previously reported ADMET EP random models, our ADMET EH models show broad endotherms at lower comonomer content than their counterpart chain-growth-based materials. For example, random copolymers made using chain-growth chemistry with greater than 5% 1-hexene incorporation generate the same type of broad curves shown here for **EH-**

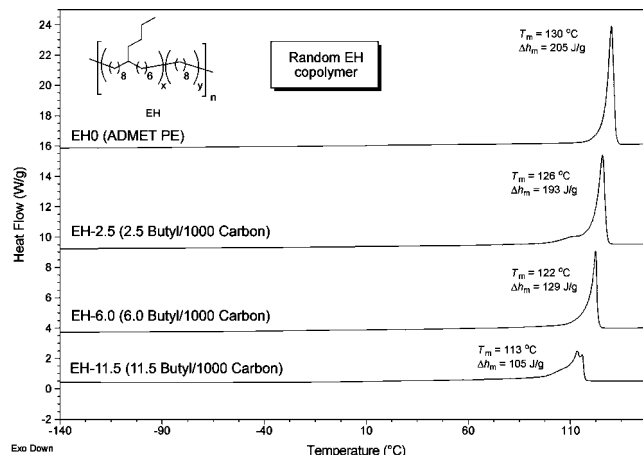


**Figure 11.** DSC profile for ADMET polymers: **EH0**, **EH-2.5**, **EH-6.0**, and **EH-11.5**.

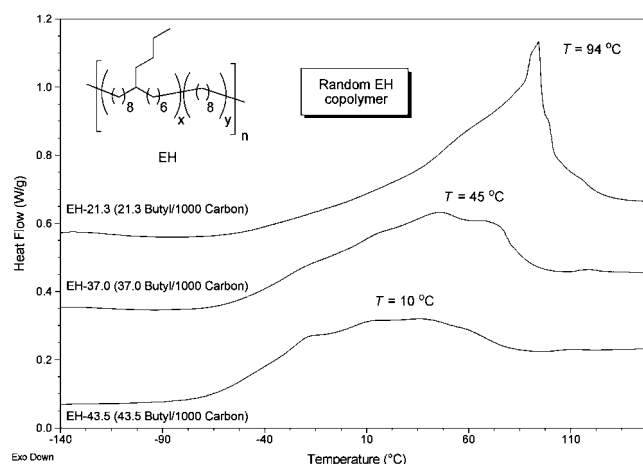


**Figure 12.** DSC profile for ADMET polymers: **EH-21.3**, **EH-37.0**, and **EH-43.5**.

**11.5** and higher.<sup>4,39</sup> However, **EH-11.5** copolymer produced by ADMET exhibits this broad melting at lower branch density ( $\sim 3\%$  1-hexene).

Figure 12 shows the DSC profiles for irregularly sequenced EH model copolymers possessing higher branch content, **EH-21.3**, **EH-37.0**, and **EH-43.5**. As expected, increasing the branch content along the PE backbone results in broadening of the endotherms. In addition, these copolymers have very indistinct  $T_m$ 's, an indication that, along with branch identity, branch distribution plays a significant role in determining the final thermal properties of the material. This observation is very evident when a copolymer with precisely spaced branches is compared to an irregular copolymer with the same total branch content. Figure 13 shows the DSC's for **EH-43.5** and **EH21**, which are EH models containing 43.5 and 48 butyl branches per 1000 backbone carbons, respectively. While **EH-43.5** shows a broad melting endotherm due to the irregularity in placing butyl branches along the PE backbone, **EH21** shows a sharp melting transition because of the higher degree of crystallinity imparted to the tertiary structure by the evenly spaced primary structure. Because ADMET chemistry results in known primary structures, we are able to manipulate the tertiary structure of the EH copolymers simply by choosing the correct monomer or comonomer. Materials with a wide range of thermal properties, from semicrystalline to fully amorphous, can be prepared simply by control of monomer architecture, without manipulation of external conditions, such as high temperature, pressure, or irradiation.

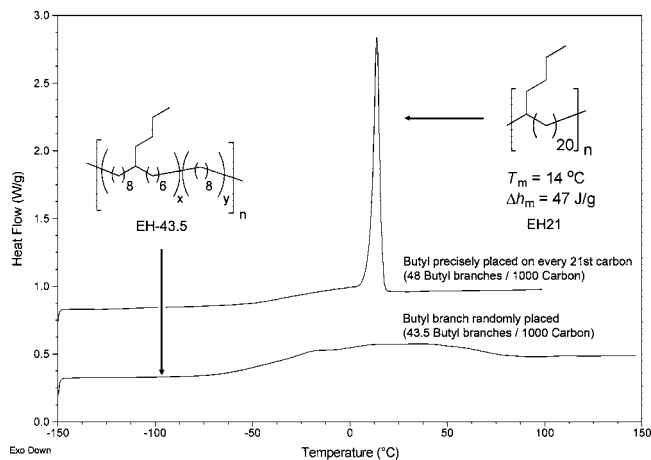


**Figure 13.** DSC profile for precisely sequenced ADMET copolymer **EH21** (48 branches/1000 backbone carbons) and irregularly sequenced **EH-43.5** ADMET copolymer (43.5 branches/1000 backbone carbons).

## Conclusions

Acyclic diene metathesis polymerization has proven to produce well-defined primary polyethylene structures. ADMET allows the intentional incorporation of “defects” regularly or irregularly placed along the polyethylene main chain. Structural and thermal study of ADMET model containing butyl branches (ethylene/1-hexene (EH) copolymers) reveals unique properties never observed for EH copolymers made via chain-propagation chemistry. Thus, the ADMET EH copolymers may be considered as a new class of polyethylene. Analogous to observations on previously reported model copolymers (EP, EB, and EO), increasing the amount of comonomer content, 1-hexene, has a pronounced lowering effect on the enthalpy of melting and peak melting transition of such materials. Moreover, manipulation of the primary structure by simple choice of monomer or comonomer architecture makes it possible to form PE materials with a wide range of properties, from semicrystalline to amorphous. Although in the past synthesis of alkyl  $\alpha,\omega$ -diene monomers has required many synthetic steps affording only low yields, production of monomers in two synthetic steps in quantitative yields is now possible using alkylation/decyanation chemistry. Our work in this area continues, focusing on much longer defect-to-defect spacing and a variety of bulkier and longer branch identities. By creating a complete catalogue of polymers with precise and irregular alkyl branch placement, we aim to understand the intriguing physical and chemical behavior of polyethylene-based materials.

## Experimental Section

**Instrumentation and Analysis.** All  $^1\text{H}$  NMR (300 MHz) and  $^{13}\text{C}$  NMR (75 MHz) spectra were recorded in  $\text{CDCl}_3$  unless otherwise stated. Chemical shifts were referenced to residual signals from  $\text{CDCl}_3$  (7.27 ppm for  $^1\text{H}$ , 77.23 ppm for  $^{13}\text{C}$ ) with 0.03% v/v TMS as an internal reference. The NMR splitting patterns are designated as follows: s, singlet; d, doublet; t, triplet; m, multiplet; and br, broad signal. For each  $^1\text{H}$  NMR spectrum, 160 transients were coaveraged using a  $90^\circ$  acquisition pulse and a total relaxation delay of 10.8 s. All spectra were Fourier transformed to 64K complex points with line broadening of 0.2 Hz. The chemical shift scale was referenced to the residual tetrachloroethane ( $\text{TCE}-d_2$ ) protons at  $\delta$  5.98 ppm. Likewise, for each  $^{13}\text{C}$  NMR spectrum, 4000 transients were coaveraged, using a  $90^\circ$  acquisition pulse with full decoupling to obtain optimal nuclear Overhauser enhancement. Broadband decoupling was performed with WALTZ-16 modulation. A total relaxation delay time of 20.9 s was employed. The spectra were Fourier transformed to 64K points, with 1 Hz line broadening.

Analysis of samples by gas chromatography (GC) was performed on a gas chromatograph, equipped with a flame ionization detector, using a capillary column coated with 5% diphenyl–95% dimethylpolysiloxane. High-resolution mass spectrometry (HRMS) was performed using a mass spectrometer in the electron ionization (EI) mode. The mass resolution was  $\sim 6000$  for EI measured at full width half-maximum (fwhm) in the high-resolution detection mode. Thin layer chromatography (TLC) was used to monitor all reactions and was performed on aluminum plates coated with silica gel (250  $\mu\text{m}$  thickness). TLC plates were developed to produce a visible signature by one of the following: ultraviolet light, iodine, vanillin,  $\text{KMnO}_4$ , or phosphomolybdic acid. Flash column chromatography was performed using ultrapure silica gel (40–63  $\mu\text{m}$ , 60 Å pore size). All reactions were performed in flame-dried glassware under argon unless otherwise stated.

Gel permeation chromatography (GPC) was performed using an internal differential refractive index detector (DRI), internal differential viscosity detector (DP), and a Precision 2 angle light scattering detector (LS). The light scattering signal was collected at a  $15^\circ$  angle, and the three in-line detectors were operated in series in the order of LS-DRI-DP. The chromatography was performed at  $45^\circ\text{C}$  using two tandem columns (10  $\mu\text{m}$  PD, 7.8 mm ID, 300 mm total length) with HPLC grade tetrahydrofuran as the mobile phase at a flow rate of 1.0 mL/min. Injections were made at 0.05–0.07% w/v sample concentration using a 322.5  $\mu\text{L}$  injection volume. In the case of universal calibration, retention times were calibrated versus narrow-range molecular weight polystyrene standards. All standards were selected to produce  $M_p$  or  $M_w$  values well beyond the expected polymer's range. The Precision LS was calibrated using narrow-range polystyrene standard having an  $M_w = 65\,500$  g/mol.

Fourier transform infrared (FT-IR) spectroscopy was carried out for monomers as well as unsaturated and saturated polymers. Monomers were prepared by droplet deposition and sandwiched between two KCl salt plates. Unsaturated and hydrogenated polymer samples were prepared by solution-casting a thin film from tetrachloroethylene onto a KCl salt plate.

Differential scanning calorimetry (DSC) was performed using a DSC equipped with a controlled cooling accessory at a heating rate of  $10^\circ\text{C}/\text{min}$  unless otherwise specified. Calibrations were made using indium and freshly distilled *n*-octane as the standards for peak temperature transitions and indium for the enthalpy standard. All samples were prepared in hermetically sealed pans (5–10 mg/sample) and were run using an empty pan as a reference and empty cells as a subtracted baseline. The samples were scanned for multiple cycles to remove recrystallization differences between the samples, and the results reported are from the third scan in the cycle. Although all samples were thermally scanned from  $-150$  to  $150^\circ\text{C}$ , in some cases the DSC plots were scaled differently for better visualization.

**Materials.** Chemicals were purchased from the Aldrich Chemical Co. and used as received unless otherwise noted. Grubbs first-generation catalyst, bis(tricyclohexylphosphine)benzylidineruthenium(IV) dichloride, was obtained from Materia, Inc., and stored in an argon-filled drybox prior to use. Wilkinson's rhodium hydrogenation catalyst  $\text{RhCl}(\text{PPh}_3)_3$  was purchased from Strem Chemical and used as received. Tetrahydrofuran (THF) and xylenes were freshly distilled from Na/K alloy using benzophenone as the indicator. The hexanenitrile and alkenyl bromide starting materials, as well as hexamethylphosphoramide, triethylamine, and 1,9-decadiene were distilled over  $\text{CaH}_2$ .

**General Monomer Synthesis.** Monomers **4a** and **4b** were synthesized according to previously published procedures.<sup>26,27</sup> A modification of the previously reported methodology was used for the synthesis of monomer **10**, 5,10-diallyltetradecane.

**Synthesis and Characterization of 5,10-Diallyltetradecane (10).** A 1 M solution of hexanenitrile (2.136 g, 22 mmol) in dry THF (17.8 mL) was prepared in a three-necked round bottomed flask equipped with a stir bar and argon inlet adapter. The solution was cooled to  $-78^\circ\text{C}$ , and a freshly prepared solution of lithium diisopropylamide (LDA) (2.18 g, 22 mmol) in THF (21.5 mL) was



added via cannula transferred. The mixture was warmed to 0 °C, stirred for 30 min, and then cooled to -78 °C. The alkenylating agent, 3-bromoprop-1-ene (**6**) (2.639 g, 22 mmol), was added at -78 °C and then stirred at 0 °C for 30 min. The mixture was gradually warmed to room temperature and stirred for 2 h. The reaction was quenched with water (100 mL), extracted three times with ether (200 mL), and washed with brine (50 mL). After drying over MgSO<sub>4</sub>, the solution was filtered, concentrated by rotary evaporation, and purified by flash column chromatography (5% v/v ethyl acetate/hexane). After purification, 3.011 g (99% yield) of a pale yellow liquid was collected, 2-allylhexanenitrile (**7**). A 1 M solution of **7** (3.011 g, 22 mmol) in dry THF (17.8 mL) was prepared in a three-necked round bottomed flask equipped with a stir bar and argon inlet adaptor. The solution was cooled to -78 °C, and a freshly prepared solution of lithium diisopropylamide (LDA) (2.18 g, 22 mmol) in THF (21.5 mL) was added via cannula transferred. The mixture was warmed to 0 °C, stirred for 30 min, and then cooled to -78 °C. 1,4-Dibromobutane (4.706 g, 22 mmol) was added at -78 °C and then stirred at 0 °C for 30 min. The mixture was gradually warmed to room temperature and stirred for an additional 2 h. The reaction was quenched with water (100 mL), extracted three times with ether (200 mL), and washed with brine (50 mL). After drying over MgSO<sub>4</sub>, the solution was filtered, concentrated by rotary evaporation, and purified by flash column chromatography (5% v/v ethyl acetate/hexane). After purification, 7.20 g (99% yield) of a pale yellow liquid was collected, 2,7-diallyl-2,7-dibutyloctanedinitrile (**9**). The following spectral properties were observed: <sup>1</sup>H NMR (CDCl<sub>3</sub>): δ (ppm) 0.93 (t, 6H, CH<sub>3</sub>), 1.30–1.60 (m, 20H), 2.32 (d, 4H), 5.20 (m, 4H, vinyl CH<sub>2</sub>), 5.82 (m, 2H, vinyl CH). <sup>13</sup>C NMR (CDCl<sub>3</sub>): δ (ppm) 14.06, 22.97, 24.80, 26.65, 35.94, 36.08, 40.56, 40.64, 120.05, 123.69, 131.97. EI/HRMS: [M]<sup>+</sup> calculated for C<sub>22</sub>H<sub>36</sub>N<sub>2</sub>: 328.2878; found: 328.2876. Elemental analysis calculated for C<sub>22</sub>H<sub>36</sub>N<sub>2</sub>: 80.43 C, 11.04 H, 8.53 N; found: 80.40 C, 11.06 H, 8.51 N.

Decyanation of compound **9** was carried out using potassium metal (6.01 g, 154 mmol). HMPA (19.891 g, 111 mmol) and ether (185 mL) were transferred to a three-neck round bottomed flask equipped with a stir bar, addition funnel, and argon inlet adaptor. A solution of 2,7-diallyl-2,7-dibutyloctane-dinitrile (**9**) (7.20 g, 22 mmol) and *t*-BuOH (4.15 g, 56 mmol) in ether (130 mL) was added dropwise to the reactor and stirred for 3 h at 0 °C. The reaction was monitored by TLC plate using 5% ethyl acetate in hexane. When no trace of starting material was observed by TLC, the remaining excess of unreacted potassium was removed from the reaction flask. The reaction was quenched with water (20 mL), extracted three times with ether (600 mL), and washed with brine (150 mL). After drying over MgSO<sub>4</sub>, the solution was filtered, concentrated by rotary evaporation, and purified by flash column chromatography (hexane). After purification, 6.10 g (99% yield) of 5,10-diallyltetradecane (**10**) was obtained as a colorless liquid. The following spectral properties were observed: <sup>1</sup>H NMR (CDCl<sub>3</sub>): δ (ppm) 0.90 (t, 6H), 1.16–1.40 (m, 22H), 2.02 (t, 4H), 4.95 (m, 4H), 5.74 (m, 2H). <sup>13</sup>C NMR (CDCl<sub>3</sub>): δ (ppm) 14.41, 23.41, 26.88, 29.20, 29.44, 30.22, 33.60, 33.90, 34.07, 37.59, 114.30, 139.49. EI/HRMS: [M]<sup>+</sup> calculated for C<sub>20</sub>H<sub>38</sub>: 278.2974; found: 278.2978. Elemental analysis calculated for C<sub>20</sub>H<sub>38</sub>: 86.25 C, 13.75 H; found: 86.23 C, 13.76 H.

**General Polymerization Conditions.** All glassware was flame-dried under vacuum prior to use. Monomers **4a**, **4b**, **10**, and **11** were dried over K mirror and degassed prior to polymerization. All metathesis reactions were initiated in the bulk, inside an argon atmosphere drybox. For the case of homopolymerization, monomers **4a**, **4b**, and **10** were each placed in a 50 mL round-bottomed flask equipped with a magnetic stirbar. Grubbs first-generation catalyst (400:1 monomer:catalyst) was added to the flask, and the flask was then fitted with a Schlenk adapter equipped with a vacuum valve. The reaction was monitored by formation of ethylene gas as a moderate observed bubbling. The sealed reaction vessel was removed from the drybox and immediately placed on the vacuum line. The reaction vessel was then exposed to intermittent vacuum. After 4 h, the polymerization was exposed to full vacuum (10<sup>-4</sup>

Torr) for 96 h at 45–50 °C. The reaction vessel was then cooled to room temperature and exposed to air, and 50 mL of a mixture of ethyl vinyl ether in toluene 1% v/v was added. The polymer/toluene solution was precipitated in methanol by dropwise addition of the solution to a beaker containing 1500 mL of acidic methanol (1 M HCl), yielding pure **EH5u**, **EH15u**, and **EH21u** polymers. For the case of copolymerization of monomers **4a** and **11**, monomers were weighted based on the needed molar ratios, as shown in Table 2. The mixture of monomers was placed in a 50 mL round-bottomed flask equipped with a magnetic stirbar, and Grubbs first-generation catalyst (400:1 monomer:catalyst) was added to the flask. Application of the same polymerization and purification procedure previously mentioned afforded the model copolymers **EH-2.5u–EH-43.5u**.

**Polymerization of 5,10-Diallyltetradecane (10) To Give EH5u.** After purification, 820 mg (90% yield) of material was collected. The following spectral properties were observed: <sup>1</sup>H NMR (CDCl<sub>3</sub>): δ (ppm) 0.91 (t, 7H), 1.25 (br, 23H), 1.97 (m, 4H), 5.35 (m, 2H). <sup>13</sup>C NMR (CDCl<sub>3</sub>): δ (ppm) 14.44, 23.38, 27.43, 29.23, 29.34, 33.29, 33.75, 36.95, 38.01, 129.40, 130.11. GPC data (THF vs polystyrene standards):  $\overline{M}_w$  = 21 200 g/mol; PDI ( $\overline{M}_w/\overline{M}_n$ ) = 1.7.

**Polymerization of 9-Butylheptadeca-1,16-diene (4a) To Give EH15u.** After precipitation, 860 mg (93% yield) of material was collected. The following spectral properties were observed: <sup>1</sup>H NMR (CDCl<sub>3</sub>): δ (ppm) 0.90 (t, 3H), 1.23 (br, 29H), 1.98 (m, 4H), 5.40 (m, 2H). <sup>13</sup>C NMR (CDCl<sub>3</sub>): δ (ppm) 14.43, 23.41, 26.92, 29.19, 29.49, 29.62, 29.95, 30.26, 32.88, 33.59, 33.93, 37.61, 130.12, 130.58. GPC data (THF vs polystyrene standards):  $\overline{M}_w$  = 47 600 g/mol; PDI ( $\overline{M}_w/\overline{M}_n$ ) = 1.9.

**Polymerization of 12-Butyltricos-1,22-diene (4b) To Give EH21u.** After precipitation, 980 mg (91% yield) of material was collected. The following spectral properties were observed: <sup>1</sup>H NMR (CDCl<sub>3</sub>): δ (ppm) 0.90 (t, 3H), 1.27 (br, 34H), 1.98 (m, 4H), 5.39 (m, 2H). <sup>13</sup>C NMR (CDCl<sub>3</sub>): δ (ppm) 14.42, 23.41, 26.96, 29.20, 29.44, 29.79, 29.92, 29.97, 30.41, 32.86, 33.60, 33.95, 37.62, 130.11, 130.57. GPC data (THF vs polystyrene standards):  $\overline{M}_w$  = 41 500 g/mol; PDI ( $\overline{M}_w/\overline{M}_n$ ) = 1.8.

**Copolymerization of 9-Butylheptadeca-1,16-diene (4a) and 1,9-Decadiene (11) To Give EH-2.5u.** After precipitation, 2.501 g (93% yield) of material was collected. The following spectral properties were observed: <sup>1</sup>H NMR (CDCl<sub>3</sub>): δ (ppm) 0.90 (t, 0.07H), 1.30 (br, 8H), 1.98 (m, 4H), 5.39 (m, 2H). <sup>13</sup>C NMR (CDCl<sub>3</sub>): δ (ppm) 14.25, 23.23, 26.73, 29.01, 29.29, 29.68, 29.75, 30.23, 32.69, 33.41, 33.73, 37.41, 129.90, 130.40. GPC data (THF vs polystyrene standards):  $\overline{M}_w$  = 40 100 g/mol; PDI ( $\overline{M}_w/\overline{M}_n$ ) = 1.8.

**Copolymerization of 9-Butylheptadeca-1,16-diene (4a) and 1,9-Decadiene (11) To Give EH-6.0u.** After precipitation, 2.027 g (89% yield) of material was collected. The following spectral properties were observed: <sup>1</sup>H NMR (CDCl<sub>3</sub>): δ (ppm) 0.90 (t, 0.2H), 1.30 (br, 9H), 1.98 (m, 4H), 5.39 (m, 2H). <sup>13</sup>C NMR (CDCl<sub>3</sub>): δ (ppm) 14.25, 23.23, 26.73, 29.01, 29.29, 29.68, 29.75, 30.23, 32.69, 33.41, 33.73, 37.41, 129.90, 130.40. GPC data (THF vs polystyrene standards):  $\overline{M}_w$  = 39 500 g/mol; PDI ( $\overline{M}_w/\overline{M}_n$ ) = 1.7.

**Copolymerization of 9-Butylheptadeca-1,16-diene (4a) and 1,9-Decadiene (11) To Give EH-11.5u.** After precipitation, 1.875 g (91% yield) of material was collected. The following spectral properties were observed: <sup>1</sup>H NMR (CDCl<sub>3</sub>): δ (ppm) 0.90 (t, 0.5H), 1.30 (br, 10H), 1.98 (m, 4H), 5.39 (m, 2H). <sup>13</sup>C NMR (CDCl<sub>3</sub>): δ (ppm) 14.25, 23.23, 26.73, 29.01, 29.29, 29.68, 29.75, 30.23, 32.69, 33.41, 33.73, 37.41, 129.90, 130.40. GPC data (THF vs polystyrene standards):  $\overline{M}_w$  = 38 700 g/mol; PDI ( $\overline{M}_w/\overline{M}_n$ ) = 1.6.

**Copolymerization of 9-Butylheptadeca-1,16-diene (4a) and 1,9-Decadiene (11) To Give EH-21.3u.** After precipitation, 1.572 g (95% yield) of material was collected. The following spectral properties were observed: <sup>1</sup>H NMR (CDCl<sub>3</sub>): δ (ppm) 0.90 (t, 1.3H), 1.30 (br, 14H), 1.98 (m, 4H), 5.39 (m, 2H). <sup>13</sup>C NMR (CDCl<sub>3</sub>): δ (ppm) 14.25, 23.23, 26.73, 29.01, 29.29, 29.68, 29.75,

30.23, 32.69, 33.41, 33.73, 37.41, 129.90, 130.40. GPC data (THF vs polystyrene standards):  $\bar{M}_w = 48\,400$  g/mol; PDI ( $\bar{M}_w/\bar{M}_n$ ) = 1.6.

**Copolymerization of 9-Butylheptadeca-1,16-diene (4a) and 1,9-Decadiene (11) To Give EH-37.0u.** After precipitation, 1.350 g (91% yield) of material was collected. The following spectral properties were observed:  $^1\text{H}$  NMR ( $\text{CDCl}_3$ ):  $\delta$  (ppm) 0.90 (t, 2.2H), 1.30 (br, 20H), 1.98 (m, 4H), 5.39 (m, 2H).  $^{13}\text{C}$  NMR ( $\text{CDCl}_3$ ):  $\delta$  (ppm) 14.25, 23.23, 26.73, 29.01, 29.29, 29.68, 29.75, 30.23, 32.69, 33.41, 33.73, 37.41, 129.90, 130.40. GPC data (THF vs polystyrene standards):  $\bar{M}_w = 37\,500$  g/mol; PDI ( $\bar{M}_w/\bar{M}_n$ ) = 1.8.

**Copolymerization of 9-Butylheptadeca-1,16-diene (4a) and 1,9-Decadiene (11) To Give EH-43.5u.** After precipitation, 1.170 g (88% yield) of material was collected. The following spectral properties were observed:  $^1\text{H}$  NMR ( $\text{CDCl}_3$ ):  $\delta$  (ppm) 0.90 (t, 3H), 1.30 (br, 25H), 1.98 (m, 4H), 5.39 (m, 2H).  $^{13}\text{C}$  NMR ( $\text{CDCl}_3$ ):  $\delta$  (ppm) 14.25, 23.23, 26.73, 29.01, 29.29, 29.68, 29.75, 30.23, 32.69, 33.41, 33.73, 37.41, 129.90, 130.40. GPC data (THF vs polystyrene standards):  $\bar{M}_w = 38\,400$  g/mol; PDI ( $\bar{M}_w/\bar{M}_n$ ) = 1.8.

**General Hydrogenation Methodology Using Wilkinson's Catalyst.** Hydrogenation was performed using a 150 mL high-pressure stainless steel reaction vessel equipped with a glass liner, temperature probe, pressure gauge, and a paddle wheel stirrer. A solution of unsaturated polymer (EH15u or EH21u) (~1.0 g) was dissolved in toluene (100 mL), followed by degasification by bubbling nitrogen gas into the stirred solution for 30 min. Wilkinson's catalyst (3.7 mg, 4  $\mu\text{mol}$ ) [ $\text{RhCl}(\text{PPh}_3)_3$ ] was added to the solution, and the glass liner was placed into the bomb and then sealed. The bomb was charged with hydrogen gas to 400 psi, and the mixture was stirred for 24 h at 80 °C followed by 48 h at 100 °C. Upon cooling to room temperature, the resultant polymer solution was precipitated into acidic methanol (1 M HCl), filtered, and dried, affording saturated polymers EH15 and EH21.

**Hydrogenation of EH15u To Give EH15.** After precipitation, 855 mg (99% yield) of material was collected. The following spectral properties were observed:  $^1\text{H}$  NMR ( $\text{CDCl}_3$ ):  $\delta$  (ppm) 0.90 (t, 3H), 1.27 (br, 31H).  $^{13}\text{C}$  NMR ( $\text{CDCl}_3$ ):  $\delta$  (ppm) 14.39, 23.40, 26.95, 29.20, 29.96, 30.40, 33.63, 33.95, 37.62. GPC data (THF vs polystyrene standards):  $\bar{M}_w = 48\,100$  g/mol; PDI ( $\bar{M}_w/\bar{M}_n$ ) = 1.9. DSC results: melting temperature data:  $T_m = -33$  °C,  $\Delta h_m = 13$  J/g and  $T_m = -53$  °C.

**Hydrogenation of EH21u To Give EH21.** After precipitation, 973 mg (99% yield) of material was collected. The following spectral properties were observed:  $^1\text{H}$  NMR ( $\text{CDCl}_3$ ):  $\delta$  (ppm) 0.90 (t, 3H), 1.27 (br, 47H).  $^{13}\text{C}$  NMR ( $\text{CDCl}_3$ ):  $\delta$  (ppm) 14.43, 23.42, 24.49, 26.95, 29.21, 29.97, 30.41, 33.62, 33.94, 37.61. GPC data (THF vs polystyrene standards):  $\bar{M}_w = 40\,300$  g/mol; PDI ( $\bar{M}_w/\bar{M}_n$ ) = 1.7. DSC results: melting temperature data:  $T_m = 14$  °C,  $\Delta h_m = 47$  J/g.

**General Hydrogenation Methodology Using Diimide.** This method was applied for the saturation of polymer EH5u and copolymers EH-2.5 through EH-43.5 due to solubility issues that were eventually overcome. A solution of unsaturated polymer (~1.0 g) was dissolved in xylenes (30 mL) in a 350 mL three-neck round bottomed flask. Tripropylamine (3.79 g, 26.3 mmol) was added via syringe followed by addition of *p*-toluenesulfonylhydrazide (4.33 g, 23.3 mmol) using a powder funnel. The reaction mixture was heated to 135 °C for 2 h. The reaction was monitored by the produced nitrogen observed through a mineral oil bubbler. When production of nitrogen gas ceased, the solution was cooled to room temperature, and a second batch of tripropylamine (3.79 g, 26.3 mmol) and *p*-toluenesulfonylhydrazide (4.33 g, 23.3 mmol) was added. The reaction mixture was heated to 135 °C for 2 h, and its performance was monitored by the evolution of nitrogen gas. Precipitation of the crude mixtures into acidic methanol (1 M HCl) followed by filtration afforded the saturated EH5 polymer and copolymers EH-2.5 through EH-43.5.

**Hydrogenation of EH5u To Give EH5.** After precipitation, 817 mg (99% yield) of material was collected. The following spectral properties were observed:  $^1\text{H}$  NMR ( $\text{CDCl}_3$ ):  $\delta$  (ppm) 0.90 (t, 3H),

1.27 (br, 14H).  $^{13}\text{C}$  NMR ( $\text{CDCl}_3$ ):  $\delta$  (ppm) 14.55, 23.55, 27.58, 29.37, 33.77, 34.15, 37.81. GPC data (THF vs polystyrene standards):  $\bar{M}_w = 20\,800$  g/mol; PDI ( $\bar{M}_w/\bar{M}_n$ ) = 1.8. DSC results: glass transition temperature data:  $T_g = -73$  °C,  $\Delta C_p = 0.63$  J/g °C.

**Hydrogenation of EH-2.5u To Give EH-2.5.** After precipitation, 2.489 g (99% yield) of material was collected. The following spectral properties were observed:  $^1\text{H}$  NMR ( $\text{TCE}-d_2$ ):  $\delta$  (ppm) 0.92 (t,  $\text{CH}_3$ , 3H), 1.19 and 1.34 (br,  $\text{CH}_2$ , 129H).  $^{13}\text{C}$  NMR ( $\text{TCE}-d_2$ ):  $\delta$  (ppm) 14.29, 14.39, 22.94, 23.40, 26.95, 29.20, 29.60, 29.99, 30.40, 32.22, 33.63, 33.95, 37.62. GPC data (THF vs polystyrene standards):  $\bar{M}_w = 39\,800$  g/mol; PDI ( $\bar{M}_w/\bar{M}_n$ ) = 1.8. DSC results: melting temperature data:  $T_m = 126$  °C,  $\Delta h_m = 193$  J/g.

**Hydrogenation of EH-6.0u To Give EH-6.0.** After precipitation, 1.993 g (98% yield) of material was collected. The following spectral properties were observed:  $^1\text{H}$  NMR ( $\text{TCE}-d_2$ ):  $\delta$  (ppm) 0.92 (t,  $\text{CH}_3$ , 3H), 1.19 and 1.34 (br,  $\text{CH}_2$ , 93H).  $^{13}\text{C}$  NMR ( $\text{TCE}-d_2$ ):  $\delta$  (ppm) 14.29, 14.39, 22.94, 23.40, 26.95, 29.20, 29.60, 29.99, 30.40, 32.22, 33.63, 33.95, 37.62. GPC data (THF vs polystyrene standards):  $\bar{M}_w = 40\,700$  g/mol; PDI ( $\bar{M}_w/\bar{M}_n$ ) = 1.6. DSC results: melting temperature data:  $T_m = 122$  °C,  $\Delta h_m = 129$  J/g.

**Hydrogenation of EH-11.5u To Give EH-11.5.** After precipitation, 1.868 g (99% yield) of material was collected. The following spectral properties were observed:  $^1\text{H}$  NMR ( $\text{TCE}-d_2$ ):  $\delta$  (ppm) 0.92 (t,  $\text{CH}_3$ , 3H), 1.19 and 1.34 (br,  $\text{CH}_2$ , 76H).  $^{13}\text{C}$  NMR ( $\text{TCE}-d_2$ ):  $\delta$  (ppm) 14.29, 14.39, 22.94, 23.40, 26.95, 29.20, 29.60, 29.99, 30.40, 32.22, 33.63, 33.95, 37.62. GPC data (THF vs polystyrene standards):  $\bar{M}_w = 37\,800$  g/mol; PDI ( $\bar{M}_w/\bar{M}_n$ ) = 1.8. DSC results: melting temperature data:  $T_m = 113$  °C,  $\Delta h_m = 105$  J/g.

**Hydrogenation of EH-21.3u To Give EH-21.3.** After precipitation, 1.469 g (93% yield) of material was collected. The following spectral properties were observed:  $^1\text{H}$  NMR ( $\text{TCE}-d_2$ ):  $\delta$  (ppm) 0.92 (t,  $\text{CH}_3$ , 3H), 1.19 and 1.34 (br,  $\text{CH}_2$ , 50H).  $^{13}\text{C}$  NMR ( $\text{TCE}-d_2$ ):  $\delta$  (ppm) 14.29, 14.39, 22.94, 23.40, 26.95, 29.20, 29.60, 29.99, 30.40, 32.22, 33.63, 33.95, 37.62. GPC data (THF vs polystyrene standards):  $\bar{M}_w = 45\,100$  g/mol; PDI ( $\bar{M}_w/\bar{M}_n$ ) = 1.6. DSC results: melting temperature data:  $T_m = 94$  °C,  $\Delta h_m = 95$  J/g.

**Hydrogenation of EH-37.0u To Give EH-37.0.** After precipitation, 1.280 g (95% yield) of material was collected. The following spectral properties were observed:  $^1\text{H}$  NMR ( $\text{TCE}-d_2$ ):  $\delta$  (ppm) 0.92 (t,  $\text{CH}_3$ , 3H), 1.19 and 1.34 (br,  $\text{CH}_2$ , 42H).  $^{13}\text{C}$  NMR ( $\text{TCE}-d_2$ ):  $\delta$  (ppm) 14.29, 14.39, 22.94, 23.40, 26.95, 29.20, 29.60, 29.99, 30.40, 32.22, 33.63, 33.95, 37.62. GPC data (THF vs polystyrene standards):  $\bar{M}_w = 38\,100$  g/mol; PDI ( $\bar{M}_w/\bar{M}_n$ ) = 1.7. DSC results: melting temperature data:  $T_m = 45$  °C,  $\Delta h_m = 93$  J/g.

**Hydrogenation of EH-43.5u To Give EH-43.5.** After precipitation, 1.152 g (98% yield) of material was collected. The following spectral properties were observed:  $^1\text{H}$  NMR ( $\text{TCE}-d_2$ ):  $\delta$  (ppm) 0.92 (t,  $\text{CH}_3$ , 3H), 1.19 and 1.34 (br,  $\text{CH}_2$ , 33H).  $^{13}\text{C}$  NMR ( $\text{TCE}-d_2$ ):  $\delta$  (ppm) 14.29, 14.39, 22.94, 23.40, 26.95, 29.20, 29.60, 29.99, 30.40, 32.22, 33.63, 33.95, 37.62. GPC data (THF vs polystyrene standards):  $\bar{M}_w = 37\,300$  g/mol; PDI ( $\bar{M}_w/\bar{M}_n$ ) = 1.8. DSC results: melting temperature data:  $T_m = 10$  °C,  $\Delta h_m = 85$  J/g.

**Acknowledgment.** The authors express thanks to the National Science Foundation (NSF), the Army Research Office (ARO) for catalyst support, and to Kathryn R. Williams for editorial contributions to this manuscript.

## References and Notes

- (1) Univation Technologies - Market Information, <http://www.univation.com>.
- (2) McKnight, A. L.; Waymouth, R. M. *Chem. Rev.* **1998**, *98*, 2587–2598.
- (3) Muller, A. J.; Hernandez, Z. H.; Arnal, M. L.; Sanchez, J. J. *Polym. Bull.* **1997**, *39*, 465–472.
- (4) Czaja, K.; Sacher, B.; Bialek, M. *J. Therm. Anal. Calorim.* **2002**, *67*, 547–554.
- (5) James, D. E. *Encyclopedia of Polymer Science and Engineering*; Mark, H. F., Bikales, N. M., Overberger, C. G., Menges, G., Eds.; Wiley-Interscience: New York, 1985; Vol. 6, p 429.

- (6) Hadjichristidis, N.; Xenidou, M.; Iatrou, H.; Pitsikalis, M.; Poulos, Y.; Avgeropoulos, A.; Sioula, S.; Paraskeva, S.; Velis, G.; Lohse, D. J.; Schulz, D. N.; Fetters, L. J.; Wright, P. J.; Mendelson, R. A.; Garcia-Franco, C. A.; Sun, T.; Ruff, C. J. *Macromolecules* **2000**, *33*, 2424–2436.
- (7) Jokela, K.; Vaananen, A.; Torkkeli, M.; Starck, P.; Serimaa, R.; Lofgren, B.; Seppala, J. *J. Polym. Sci., Part B: Polym. Phys.* **2001**, *39*, 1860–1875.
- (8) Bracco, S.; Comotti, A.; Simonutti, R.; Camurati, I.; Sozzani, P. *Macromolecules* **2002**, *35*, 1677–1684.
- (9) Wright, K. J.; Lesser, A. J. *Macromolecules* **2001**, *34*, 3626–3633.
- (10) Gupta, P.; Wilkes, G. L.; Sukhadia, A. M.; Krishnaswamy, R. K.; Lamborn, M. J.; Wharry, S. M.; Tso, C. C.; DesLauriers, P. J.; Mansfield, T.; Beyer, F. L. *Polymer* **2005**, *46*, 8819–8837.
- (11) Peacock, A. J. *Handbook of Polyethylene: Structures, Properties, and Applications*; Marcel Dekker: New York, 2000, 534 pp.
- (12) Shan, C. L. P.; Soares, J. B. P.; Penlidis, A. *J. Polym. Sci., Part A: Polym. Chem.* **2002**, *40*, 4426–4451.
- (13) Da Silva, A. A.; Soares, J. B. P.; De Galland, G. B. *Macromol. Chem. Phys.* **2000**, *201*, 1226–1234.
- (14) Czaja, K.; Bialek, M. *Polymer* **2001**, *42*, 2289–2297.
- (15) Takaoka, T.; Ikai, S.; Tamura, M.; Yano, T. *J. Macromol. Sci., Pure Appl. Chem.* **1995**, *A32*, 83–101.
- (16) Madkour, T. M.; Goderis, B.; Mathot, V. B. F.; Reynaers, H. *Polymer* **2002**, *43*, 2897–2908.
- (17) Suhm, J.; Schneider, M. J.; Mulhaupt, R. *J. Polym. Sci., Part A: Polym. Chem.* **1997**, *35*, 735–740.
- (18) Suhm, J.; Schneider, M. J.; Mulhaupt, R. *J. Mol. Catal. A: Chem.* **1998**, *128*, 215–227.
- (19) O’Gara, J. E.; Wagener, K. B. *Makromol. Chem., Rapid Commun.* **1993**, *14*, 657–662.
- (20) Sworen, J. C.; Smith, J. A.; Berg, J. M.; Wagener, K. B. *J. Am. Chem. Soc.* **2004**, *126*, 11238–11246.
- (21) Sworen, J. C.; Wagener, K. B. *Macromolecules* **2007**, *40*, 4414–4423.
- (22) Smith, J. A.; Brzezinska, K. R.; Valenti, D. J.; Wagener, K. B. *Macromolecules* **2000**, *33*, 3781–3794.
- (23) Baughman, T. W.; Sworen, J. C.; Wagener, K. B. *Macromolecules* **2006**, *39*, 5028–5036.
- (24) Baughman, T. W.; Wagener, K. B. *Metathesis Polym.* **2005**, *176*, 1–42.
- (25) Rojas, G.; Berda, E. B.; Wagener, K. B. *Polymer* **2008**, *49*, 2985–2995.
- (26) Rojas, G.; Baughman, T. W.; Wagener, K. B. *Synth. Commun.* **2007**, *37*, 3923–3931.
- (27) Rojas, G.; Wagener, K. B. *J. Org. Chem.* **2008**, *73*, 4962–4970.
- (28) Tashiro, K.; Sasaki, S.; Kobayashi, M. *Macromolecules* **1996**, *29*, 7460–7469.
- (29) Sworen, J. C.; Smith, J. A.; Wagener, K. B.; Baugh, L. S.; Rucker, S. P. *J. Am. Chem. Soc.* **2003**, *125*, 2228–2240.
- (30) Pracella, M.; D’Alessio, A.; Giaiacopi, S.; Galletti, A. R.; Carlini, C.; Sbrana, G. *Macromol. Chem. Phys.* **2007**, *208*, 1560–1571.
- (31) Rueda, D. R.; Baltacalleja, F. J.; Hidalgo, A. *J. Polym. Sci., Part B: Polym. Phys.* **1977**, *15*, 2027–2031.
- (32) Ke, B. *J. Polym. Sci.* **1960**, *42*, 15–23.
- (33) Zhang, F. J.; Song, M.; Lu, T. J.; Liu, J. P.; He, T. B. *Polymer* **2002**, *43*, 1453–1460.
- (34) Starck, P.; Malmberg, A.; Lofgren, B. *J. Appl. Polym. Sci.* **2002**, *83*, 1140–1156.
- (35) Pak, J.; Wunderlich, B. *Macromolecules* **2001**, *34*, 4492–4503.
- (36) Boz, E.; Ghiviriga, I.; Nemeth, A. J.; Jeon, K.; Alamo, R. G.; Wagener, K. B. *Macromolecules* **2008**, *41*, 25–30.
- (37) Krimm, S. *Fortschr. Hochpolym.-Forsch.* **1960**, *2*, S 51.
- (38) Zerbi, G. *Modern Polymer Spectroscopy*; Wiley-VCH: New York, 1999; 304 pp.
- (39) Zhang, J. W.; Li, B. G.; Fan, H.; Zhu, S. J. *J. Polym. Sci., Part A: Polym. Chem.* **2007**, *45*, 3562–3569.

MA802241S